CHEMICAL ENGINEERING SCIENCE
GENIE CHIMIQUE

VOL. 13 1960 No. 2

The condensation of a vapour by mixing with a cool gas

D. G. LEVINE* and S. K. FRIEDLANDER
Department of Chemical Engineering, The Johns Hopkins University, Baltimore 18, Maryland

(*Received* 30 *August* 1959)

Abstract—The mechanisms of condensation from a mixture of a vapour and a non-condensable gas are reviewed. A theory of condensation by mixing with a cool gas is given when the Lewis number for the condensing species is unity. The method can be used to predict whether fog formation is possible in a mixing system. An experimental system designed to test some of the theoretical conclusions is described. The apparatus permits the production of air–vapour mixtures of known and controllable temperature and concentration. Experimental data are reported for a turbulent jet containing glycerine vapour. The results indicate that vapour concentrations considerably higher than the theoretical minimum are necessary for detectable condensation in jet mixing.

Résumé—Revue du mécanisme de la condensation d'un mélange de vapeurs et de gas inertes. Théorie de la condensation par mélange dans le cas de la valeur unité pour le nombre de Lewis de la vapeur condensable ; cette méthode permet de prédire la formation éventuelle d'un brouillard dans la zone de mélange. Description d'un dispositif expérimental pour vérifier certaines des conclusions théoriques. Cet appareil permet la production et le contrôle de mélanges air-vapeur de concentrations et de températures connues. Données expérimentales pour un jet turbulent contenant de la vapeur de glycérine. Résultats montrant qu'il est nécessaire de dépasser considérablement la concentration minimum théorique pour pouvoir obtenir une condensation décelable dans le mélange par éjecteur.

Zusammenfassung—Die Mechanismen der Kondensation eines Gemisches aus einem Dampf und einem nichtkondensierbaren Gas wird betrachtet. Eine Theorie der Kondensation durch Zumischen eines kalten Gases wird für den Fall erläutert, dass die Lewis-Zahl des kondensierenden Anteils eins ist. Diese Methode kann dazu dienen vorauszusagen, ob in einem sich mischenden System eine Nebelbildung möglich ist. Ein experimentelles System wird beschrieben, das darauf angelegt ist, einige der theoretischen Schlussfolgerungen nachzuprüfen. Der Apparat gestattet, Luft-Dampf-Gemische bekannter und regelbarer Temperatur und Konzentration herzustellen. Es wird über experimentelle Ergebnisse für einen turbulenten Gas-Glycerindampf-Strahl berichtet. Die Ergebnisse zeigen, dass beträchtlich höhere Dampfkonzentrationen als das theoretische Minimum notwendig sind, um eine merkliche Kondensation in einem Düsenmischer zu erhalten.

INTRODUCTION

CONDENSATION from a mixture of a vapour and a non-condensable gas is most often produced by: (1) cooling at the boundaries when the gas flows over a cold surface; (2) adiabatic or nearly adiabatic expansion; or (3) mixing with another, cooler, gas. The first mechanism, surface cooling, produces a gross transfer of vapour to the wall; this may be accompanied by fog formation in the gas if local conditions are such that supersaturation is attained. This process has been studied by JOHNSTONE *et al.* [1] who passed mixtures of nitrogen with vapours of sulphur, *n*-butyl alcohol and water through a short condenser section. Using an approximate theoretical analysis they were able to predict in most instances whether or not fog would form in the condenser section. Their results must be regarded

*Present Address: Esso Research and Engineering Co., Linden, N.J.

as only semi-quantitative since no effort was made to measure or control the fluid mechanical situation.

In the second process, adiabatic expansion, condensation may result when the slope of the isentrope on the vapour pressure vs. temperature plot is less than the slope of the saturation curve. It is the mechanism on which the Wilson cloud chamber is based and is of controlling importance in the growth of water droplets in the atmosphere [2]. It has been studied in some detail in high-speed flow processes by passing mixtures of water vapour and air through a converging–diverging nozzle (see for example the review by Stever [3]). Supersonic velocities are attained in the diverging section where both the pressure and temperature drop rapidly in such fashion as to produce a supersaturated vapour. This process is the flow analog of the cloud chamber.

Condensation produced by expansion may take place either on foreign nuclei or as a result of self-nucleation (see for example Frenkel [4]) depending on the speed of the expansion process. In high-speed expansions in the cloud chamber or in nozzle flows, high values of the supersaturation are attained and self-nucleation dominates. In atmospheric expansion processes it is likely that foreign nuclei are most important.

The third mechanism, mixing, is the subject of this paper. When a hot condensable vapour is mixed with a cool gas, both the vapour concentration and temperature fall. The criterion for condensation is that at some point during the mixing process, the temperature drops sufficiently under the dew point to initiate stable droplet formation. The occurrence of condensation depends on the relative rates of heat and mass transfer in the mixing system. It is quite possible that a hot vapour which would condense were it at the temperature of the ambient atmosphere will not condense during mixing. As in the case of expansion condensation may take place either on foreign nuclei or by self-nucleation depending on the speed on the mixing process. If mixing is slow condensation will take place on dust particles and other suspended matter in the gas. On the other hand, rapid mixing will produce high values of the supersaturation and self-nucleation will dominate. If mixing is sufficiently rapid it is also possible for the system to pass through the two-phase region without condensation.

Despite the ubiquity of vapour mixing as a method of forming natural and artificial aerosols few theoretical or control experimental studies of the process seem to have been made. Among the most interesting is that of Amelin and Belakov [5] who measured the size distribution of drops formed when glycerine vapour was jetted into cool air. They found that the mean size of the drops decreased as gas velocity increased and concluded that self nucleation rather than condensation on foreign nuclei was predominant.

In the present paper the authors show that under certain conditions it is possible to trace the path followed by the properties (composition and temperature) of a mixing system. In addition, qualitative statements can be made as to the effect of operating variables on particle size. An experimental apparatus designed to study the phenomenon is described and data are reported for the turbulent jet mixing of glycerine–air mixtures with cool air.

The Concentration and Temperature Fields

A system typical of the type to be considered is a steam jet exhausting to the atmosphere. The onset of condensation depends on the concentration and temperature distributions in the mixing vapours. It is possible to set up the equations of energy and diffusion in a number of ways for such a system [6]. To relate the concentration and energy parameters of the mixing process most easily to the "natural" thermodynamic variables of condensation a molar basis is chosen for the equations. In the absence of condensation and of thermal and pressure diffusion the equation of conservation of species i can be written in the form:

$$n\frac{\partial y_i}{\partial t} + n\boldsymbol{v}\cdot\nabla y_i = \nabla\cdot n\,D_i\,\nabla y_i \qquad (1)$$

where the velocity $\boldsymbol{v}$ is the mean molal velocity. For a binary, D_i can be identified with the binary diffusion coefficient as defined in the

kinetic theory of gases. (See for example CHAPMAN and COWLING [7]).

In the absence of condensation an energy balance on the mixture can be written in the form

$$n\frac{\partial T}{\partial t} + n\mathbf{v}\cdot\nabla T = \nabla\cdot(k/c_p)\,\nabla T \qquad (2)$$

The most important assumptions involved in the derivation are (1) the pressure is constant throughout the system; (2) viscous dissipation can be neglected; (3) the Dufour effect (the interaction between diffusion and conduction) can be neglected; (4) the system is a perfect gas mixture; (5) the molal heat capacities of all species are equal.

Suppose a stream (or streams) of condensable vapour at a concentration y_0 and temperature T_0 mixes with gas of concentration y_∞ and temperature T_∞. New concentration and temperature variables can be defined as:

$$y' = \frac{y - y_\infty}{y_0 - y_\infty} \quad T' = \frac{T - T_\infty}{T_0 - T_\infty} \qquad (3)$$

Equations (1) and (2) become

$$n\frac{\partial y'}{\partial t} + n\mathbf{v}\cdot\nabla y' = \nabla\cdot nD\,\nabla y' \qquad (4)$$

$$n\frac{\partial T'}{\partial t} + n\mathbf{v}\cdot\nabla T' = \nabla\cdot(k/c_p)\,\nabla T' \qquad (5)$$

For the vapour jet, the boundary conditions in terms of the new variables are:

$$y' = T' = 1 \text{ over the jet orifice}$$

$$y' = T' = 0 \text{ at infinity} \qquad (6)$$

For steam–air mixtures the Lewis number, $N_{LE} = k/nDC_p$, is not far from one and practically constant over a wide range of temperatures. For most other gas mixtures it is of the order of unity. When $N_{LE} = 1$, $nD = k/C_p$ and equations (4) and (5) are of the same form; moreover the boundary conditions are identical. In principle with sufficiently accurate instruments it would be possible to measure $\mathbf{v}$ and thus determine the velocity field. With the same velocity field and identical boundary conditions the solutions to equations (4) and (5) must be the same, i.e.

$$y' = T' \text{ or } \frac{y = y_\infty}{y_0 - y_\infty} = \frac{T - T_\infty}{T_0 - T_\infty} \qquad (7)$$

This equality is independent of the geometry of the velocity field or of whether it is turbulent or laminar.

THE EQUATION OF EQUILIBRIUM

Equation (7) relates the concentration and temperature at all points in the absence of condensation. The equilibrium properties of the system are described by an equation of the Clapeyron type: For the equilibrium of a pure liquid with its vapour in a perfect gas mixture this takes the form: (see for example DENBIGH [8])

$$\left(\frac{\partial \ln y}{\partial T}\right) = \frac{\lambda}{RT^2} \qquad (8)$$

Integrating, assuming that λ is constant over the temperature range of interest, there results

$$y_s = \exp\left[-\frac{\lambda}{R}\left(\frac{1}{T} - \frac{1}{T_b}\right)\right] \qquad (9)$$

where T_b = boiling temperature at the total pressure on the system.

TRACING THE COURSE OF CONDENSATION

A plot of equation (9) – the saturation curve – is shown in Fig. 1 for glycerine vapour. The dilution of a vapour of initial properties y_0, T_0

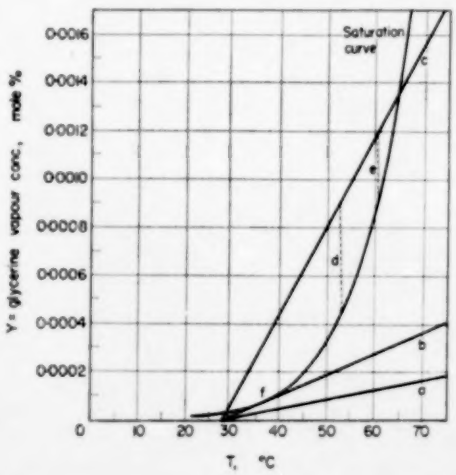

FIG. 1. The course of condensation in a mixing system.

by a vapour at y_∞, T_∞ is represented by the straight line determined by equation (7) if $N_{LE} = 1$. Each element of vapour begins at concentration y_0 and temperature T_0 and passes through the same series of states to y_∞, T_∞. The time spent in each state differs depending on the fluid mechanics of the system. Of course in a turbulent flow the concentration and temperature may momentarily increase. If the line representing the locus of states does not intersect the saturation curve, a vapour of the given initial concentration will not condense (curve *A*).

For a given initial temperature and ambient conditions there is a minimum initial concentration below which condensation cannot occur. This concentration is determined by the tangent to the saturation curve (curve *B*) and can be calculated in the following way. For simplicity it is assumed that $y_\infty = 0$. At the point of tangency, $y = y_s$, $dy/dT = dy_s/dT$ and

$$\left[\frac{T_\theta - T_\infty}{T_0 - T_\infty}\right] y_0 = \exp\left[-\frac{\lambda}{R}\left(\frac{1}{T_\theta} - \frac{1}{T_b}\right)\right] \quad (10)$$

Also

$$\frac{y_0}{T_0 - T_\infty} = \frac{\lambda}{RT_\theta^2}\exp\left[-\frac{\lambda}{R}\left(\frac{1}{T_\theta} - \frac{1}{T_b}\right)\right] \quad (11)$$

Solving simultaneously

$$RT_\theta^2 - \lambda T_\theta + \lambda T_\infty = 0 \quad (12)$$

and

$$T_\theta = \frac{\lambda}{2R}\left[1 \pm \sqrt{\frac{(1 - 4RT_\infty)}{\lambda}}\right] \quad (13)$$

Only the lower root is of interest. The criterion for condensation becomes:

$$y_0 \geq \left[\frac{T_0 - T_\infty}{T_\theta - T_\infty}\right]\exp\left[-\frac{\lambda}{R}\left(\frac{1}{T_\theta} - \frac{1}{T_b}\right)\right] \quad (14)$$

where

$$T_\theta = \frac{\lambda}{2R}\left[1 - \sqrt{\frac{(1 - 4RT_\infty)}{\lambda}}\right] \quad (15)$$

If the initial conditions are such that the system enters the saturation region nucleation and condensation may take place depending on the time spent and supersaturation attained. The maximum supersaturation occurs when the system passes through the saturation region without condensation. The path followed is still a straight line (curve *C*). The maximum value of the supersaturation can be calculated by setting its derivative with respect to T equal to zero. For $y_\infty = 0$ this is given by:

$$S_m = \left[\frac{T_m - T_\infty}{T_0 - T_\infty}\right] y_0 / \exp\left[-\frac{\lambda}{R}\left(\frac{1}{T_m} - \frac{1}{T_b}\right)\right] \quad (16)$$

The temperature at which S_m occurs is the same as that at the point of tangency (equation 15).

The initial behaviour and particle size of the condensing system will depend on the rate of mixing. If mixing is carried out slowly, condensation will take place on the foreign nuclei which happen to be present and high values of the supersaturation will never be reached (curve *E*). Particle size will be large and concentration low. If mixing is rapid, the time available for the initial nucleation and condensation will be short, and it will be possible for the system to approach the maximum value of the supersaturation where the formation of very small particles proceeds at a high rate by self-nucleation (curve *D*). Finally, if S_m is not large and if the system passes through the saturation region very quickly, it is possible that little condensation will take place at all. In any case, as mixing continues, the aerosol formed must always become unstable and tend to evaporate since the ambient atmosphere is unsaturated. However, a meta-stable state may exist if the vapour pressure of the particles is low at ambient temperature.

The effect of $N_{LE} \neq 1$ can be estimated qualitatively. For dilute mixtures of a condensable vapour with air, the thermal diffusivity is usually greater than the molecular diffusivity of the vapour and $N_{LE} > 1$. Heat diffuses more rapidly than mass and the concentration of each element of gas tends to be somewhat higher at any temperature than the value it would have assumed for $N_{LE} = 1$. Hence, a gas element follows a path concave downwards on the y vs. T plot. In the absence of condensation, the path begins at the conditions of the nozzle and ends at ambient conditions. However, the series of states traced by each element of gas differs from that of its neighbour unlike the case for $N_{LE} = 1$.

VOL 13 196

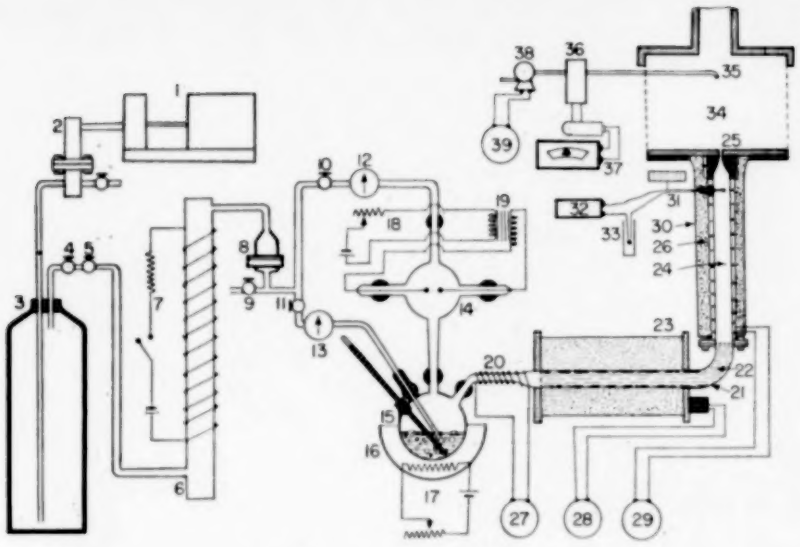

FIG. 2. Experimental equipment.

EXPERIMENTAL EQUIPMENT

To study condensation by mixing, an apparatus has been set up which generates vapour continuously under controlled conditions. A diagram of the equipment is shown in Fig. 2. Room air is filtered and compressed in a $\frac{3}{4}$ cu. ft/min air pump (1). It is refiltered (2) and passed through a surge tank (3) and control valves (4) and (5). The air is dried in a Drierite column (6) which must be regenerated periodically by the heating system (7). The air is again filtered at (8). A bleed valve at (9) may be used to adjust to various operating conditions. Valves (10) and (11) and rotameters (12) and (13) are used to regulate and measure the flow of air to the ionizer (14) and vaporizer (15) respectively. The vaporizer contains the aerosol material. It is heated to a temperature below the normal boiling point by a heater (16) which is controlled by the system (17). The ionizer is a chamber containing sealed platinum electrodes. A spark is provided from power supplied by the system (18) which consists of a 115 V a.c. supply, powerstat and 10,000 V ignition transformer (19). Ions generated to serve as condensation nuclei can be combined in the vaporizer with the hot air and vapour.

The stream from the vaporizer passes into a heating and mixing section consisting of a 14 in. length of 1 in. stainless steel pipe (21) packed with small pieces of stainless steel screen (22). The approach section to the packed tube is heated by a $\frac{1}{2}$ in. heating tape (20) controlled by a powerstat (27). The tube passes through a combustion furnace (23) and is connected by an elbow to a 25 in. length of 1 in. stainless steel pipe (24) which serves as the approach section to the nozzle (25). The nozzle is a stainless steel converging section with an orifice diameter of $\frac{1}{4}$ in. The approach section and nozzle are wrapped with a $\frac{1}{2}$ in. heating tape (26) surrounded by insulating material (30). An iron–constantan thermocouple mounted in a traversing probe (31) is located 10 cm upstream from the mouth of the nozzle. It is used to measure the temperature distribution in the approach section to the nozzle. The thermocouple leads are connected to a potentiometer (32) with an ice-bath junction (33) to establish the reference potential.

The nozzle enters the condensation chamber (34) through a transite floor. The transite roof of the chamber is fitted with an exhaust duct which leads to a blower. The side walls of the chamber are perforated to allow passage of air, but minimize drafts. The front of the chamber consists of a sheet of plexiglass for visual and photographic observation. The condensing jet may be illuminated from the side by a vertically collimated beam of light.

A sampling probe (35) is located 50 diameters downstream from the nozzle along the axis of the jet. During a run from the chamber is continuously drawn through the probe and then through a Sinclair–Phoenix forward-scattering smoke photometer (36) by a blower (38). The photocell current is read on a logarithmic amplifier (37).

Glycerine was chosen as the aerosol material since its properties are well known [10], it is easy to handle and it has been used in related studies. It is a "high boiler" and the aerosol drops can be recovered and kept for examination. The glycerine employed was reagent grade.

Experimental Procedure

A known weight of glycerine was placed in the vaporizer (15). With inlet valves (10) and (11) shut the vaporizer was heated to approximately the desired operating temperature. During this period the entire system was heated to prevent condensation in the line during the start of a run. The loss of glycerine in the boiler during this time was negligible. Next, either or both of the valves (10) and (11) were opened and the flow rates were maintained constant. The temperature in the vaporizer reached a constant value within 3–4 min. The generation system was allowed to operate in this fashion for from 4–7 hr. The average concentration of vapour in the efflux was determined from the weight loss of glycerine and the known air-flow rate.

The presence of fog in the jet was detected by the photometer (36). Before beginning a run the chamber was purged with room air and the meter (37) adjusted to zero. This adjustment showed little fluctuation from day to day. The vapour and air from the boiler were heated in the packed tube and entrance section until no condensation could be detected. A rough determination of the initial condensation point was made by rapidly lowering the nozzle temperature, T_0, until condensation was noted. The gas stream was then reheated until the meter reading returned to zero and a careful determination made by lowering the temperature slowly over a period of 30 min or more. At some point the meter reading rose sharply to values of 2–5 corresponding approximately to a 10^2–10^5 increase in mass concentration of condensed matter [9]. This point was defined as the onset of condensation. A check was made by slowly raising the temperature until the meter reading returned to zero. Within experimental error, the same point was found. At the condensation point, it was possible to observe visually occasional puffs of fog in the chamber.

Results and Discussion

When a vapour stream is mixed with cool air there are ranges of initial concentration and temperature which do not lead to condensation. This was observed in a preliminary investigation in which photographs were made of the condensing jet for various initial concentrations of glycerine in the range $y_0 = 0{\cdot}003$ per cent to $y_0 = 1{\cdot}775$ per cent. The initial temperature, T_0, was 190°C and the gas velocity was approximately 1000 cm/sec. Figs. 3 (a)–(e) show the effect of decreasing concentration of the position of the condensation zone. As y_0 decreased, this zone tended to blow off the nozzle until it disappeared completely.

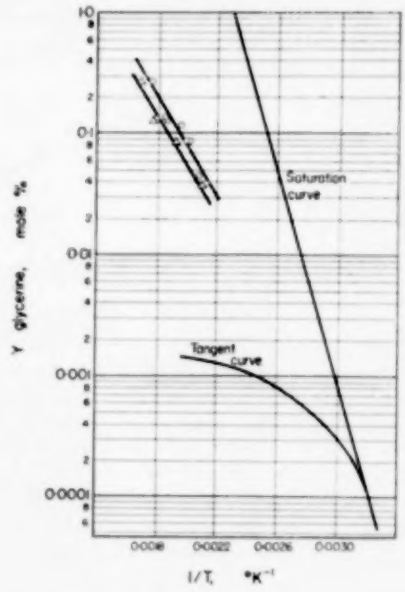

Fig. 4. Limiting conditions at nozzle for condensation in a turbulent jet: nozzle velocity ≃ 1000 cm/sec. Δ with ions. o without ions.

The experimental programme was concerned largely with investigating the limits of vapour concentration and temperature at the nozzle which lead to detectable condensation. The limits were measured for glycerine–air streams both with and without the introduction of ions. Glycerine concentrations at the nozzle ranged from 0·038 to 0·273 mole per cent and temperatures from 197°C to 292°C. In this study it was not intended to vary the gas velocity at the exit of the nozzle but values did range from 900 to 1380 cm/sec. The results are presented in Fig. 4. The region

VOL. 13 1961

VOL. 13 1961

FIG. 3. The effect of decreasing concentration on the position of the condensation zone with velocity and temperature at the nozzle held constant (the horizontal line indicates the level of the nozzle).

VOL.
13
1961

above the lines represents vapour temperatures and concentrations at the nozzle for which condensation was found in the jet. No detectable condensation took place for nozzle conditions corresponding to points in the region below the lines. The mass concentration of the fog increased sharply (about three or four orders of magnitude) when the ions were introduced. No measurement of ion concentration was made but the air velocity through the ionizer and the applied potential were kept constant in all runs.

Also shown in Fig. 4 are the saturation curve for glycerine and the tangent curve (line *B* in Fig. 1). The saturation curve is based on the data of STEDMAN [11] assuming a total pressure of 1 atm. An independent determination of the vapour pressure of glycerine has been made by FILOSOFO *et al.* [12]. Their results agree with those of STEDMAN. The results of ZIL'BERMAN-GRANOVSKAYA as reported in [10], (p. 266) do not agree with STEDMAN's measurements. The tangent curve is drawn for $T_\infty = 28°C$, $y_\infty = 0$, and a total pressure of 1 atm.

If the Lewis number were unity for glycerine–air mixtures, the tangent line would represent the lowest position along which the experimental curves could fall, and Fig. 4 would indicate that concentrations considerably in excess of the theoretical minimum values are necessary for detectable condensation. Actually, for glycerine–air mixtures $N_{LE} \simeq 3$ based on a diffusion coefficient of 0·0695 cm/sec (20°C, 1 atm) calculated from the Arnold equation. The path followed by a gas element on the y vs. T plot is concave downwards since, as discussed above, cooling occurs more rapidly than mixing. Hence even lower concentrations should be necessary at the nozzle to produce condensation for $N_{LE} = 3$ than for $N_{LE} = 1$. This strengthens the conclusion that very high supersaturations must be attained in a rapid mixing process for detectable condensation to occur. In the presence of a large amount of inert (air) the growth of nuclei, whether foreign or self-generated, probably depends on a process of local diffusion. This process is too slow to permit the growth of nuclei to a size large enough for detection by the photometer unless the local supersaturation is very high. In the absence of condensation, it is probable that most of the glycerine is dissipated molecularly or as small clusters which soon re-evaporate as mixing proceeds.

Acknowledgement—This work was supported by A. E. C. Contract at (30–1)–2165.

NOTATION

C_p = molal heat capacity
D, D_i = diffusion coefficient
k = thermal conductivity
n = molal density
N_{LE} = Lewis number $= k/n\,DC_p$
R = gas constant
S = supersaturation
t = time
T = temperature
v = molal gas velocity
y, y_i = concentration of condensible vapour, mole fraction
λ = molal latent heat of vaporization

Subscript
0 = inlet conditions
∞ = ambient conditions
θ = tangency conditions
m = maximum value
b = boiling
s = saturation curve

REFERENCES

[1] JOHNSTONE H. F., KELLEY M. D. and MCKINLEY D. L. *Industr. Engng. Chem.* 1950 **42** 2298.

[2] MASON B. J. *The Physics of Clouds.* Oxford University Press 1957.

[3] STEVER H. G. *Condensation Phenomena in High-speed Flows in Fundamentals of Gas Dynamics* (Edited by emmons H. W.). Princeton University Press, Princeton 1958.

[4] FRENKEL J. *Kinetic Theory of Gases* Chap. 7. Dover, New York 1955. (Republication of Oxford University Press edition).

[5] AMELIN A. G. and BELAKOV M. I. *Kolldid. Zh.* 1955 **17** 10.

[6] MERK H. J. *Appl. Sci. Res.* 1958 **A8** 73.

[7] CHAPMAN S. and COWLING T. G. *The Mathematical Theory of Non-uniform Gases.* Cambridge University Press 1939.

[8] DENBIGH K. *The Principles of Chemical Equilibrium* p. 202. Cambridge University Press 1955.

[9] MULLER R. H. *Analyt. Chem.* 1954 **26** 33A.

[10] MINER C. S. and DALTON N. N. (Editors) *Glycerol.* Rheinhold, New York 1953.

[11] STEDMAN D. F. *Trans. Faraday Soc.* 1938 **24** 296.

[12] FILOSOFO I., MERLIN M. and ROSTAGNI A. *Nuovo. Cim.* 1950 **7** 69.

VOL
13
1961

Chemical Engineering Science, 1960, Vol. 13, pp. 57 to 62. Pergamon Press Ltd., London. Printed in Great Britain

On laminar boundary layer flows with a rapid homogeneous chemical reaction

A. Acrivos
Department of Chemical Engineering, University of California, Berkeley

(*Received* 9 *November* 1959; *in revised form* 9 *January* 1960)

Abstract—A theoretical analysis is presented of a mass transfer process which is coupled with an instantaneous homogeneous chemical reaction between two substances. It is shown how the appropriate diffusion and energy equations for laminar boundary layer flows past arbitrary surfaces may be solved in closed form by making use of an asymptotic technique. Of particular interest is the derived expression for the rate of mass transfer, of one of the reacting species from the surface, which has the simple form

$$\mathrm{Nu} = \mathrm{Nu}_0\, C(\alpha, \lambda)$$

Nu_0 is the local Nusselt number in the absence of a chemical reaction, and $C(\alpha, \lambda)$ is a correction factor, independent of the surface geometry, which can be calculated exactly as a function only of two fluid parameters α and λ.

Résumé—Présentation de l'analyse théorique d'un processus de transfert de matrière couplé avec une réaction chimique homogène instantanée entre deux substances. On montre comment résoudre par une méthode de tangentes une expression implicite des équations convenables pour la diffusion et l'énergie pour l'écoulement laminaire de la couche limite au contact de surfaces arbitraires. Pour la vitesse de transfert d'un des réactifs au travers de la surface, on peut dériver une expression particulièrement intéressante de forme simplifiée :

$$\mathrm{Nu} = \mathrm{Nu}_0\, C(\alpha, \lambda)$$

Nu_0 étant le nombre de Nusselt local dans l'absence de réaction chimique et $C(\alpha, \lambda)$ est un facteur de correction, indépendant de la géométrie de la surface, pouvant être calculée calculée en fonction de deux paramètres du fluide α et λ.

Zusammenfassung—Eine theoretische Analyse eines Stoffübergans wird dargelegt, der mit einer rasch verlaufenden chemischen Reaktion zwischen zwei Substanzen gekoppelt ist. Es wird gezeigt, wie geeignete Diffusions- und Energiegleichungen für laminar, über beliebige Oberflächen fliessende Grenzschichten dadurch in geschlossener Form gelöst werden können, dass man eine Asymptotentechnik benutzt. Von besonderem Interesse ist der Ausdruck, der für die Massenübergangsgeschwindigkeit einer der beiden Reaktionspartner von der Oberfläche weg abgeleitet ist. Er hat die folgende Form

$$\mathrm{Nu} = \mathrm{Nu}_0\, C(\alpha, \lambda).$$

Nu_0 ist die örtliche Nusselt-Zahl unter Ausschluss der chemischen Reaktion. $C(\alpha, \lambda)$ ist ein Korrekturfaktor, der von der Gestalt der Oberfläche unabhänging ist und der als Funktion der beiden Parameter des fliessenden Mediums α und λ genau berechnet werden kann.

Introduction

Fluid mechanical phenomena involving the simultaneous transfer of matter with a chemical reaction have received a considerable amount of attention in the last few years [1, 2, 3, 4]. One of the reasons for this is that it is of some importance in a number of chemical engineering operations to be able to determine to what extent the rate of mass transfer from a surface to a moving fluid stream will be affected by the presence of a chemical reaction, either on the surface itself or in the bulk of the fluid. In the present theoretical analysis we shall deal with a special problem in this broad field. We shall consider the effect on the rate of mass transfer of a very rapid homogeneous reaction between two chemical species, and show how the solution of Friedlander and Litt [5] to the equations of diffusion and

energy, for such a reaction occurring in the laminar boundary layer on a flat plate, may be generalized to systems with an arbitrary surface geometry.

Let us visualize a typical physical set-up for such a process. A fluid containing a reactant B flows past the arbitrary surface, shown schematically in Fig. 1, which generates the other reacting species A. As an example, A might be an organic acid which is slowly dissolving from the solid surface and instantaneously reacts with a liquid stream containing a base. Or, alternatively, if the convective fluid is a gas, A might be a vapour generated from the surface either by evaporation or sublimation. In any case, since the reaction between A and B is assumed instantaneous, it is clear that the flow field will be divided into two distinct regions which, as is illustrated in Fig. 1, are separated by a reaction zone of infinitesimal thickness.

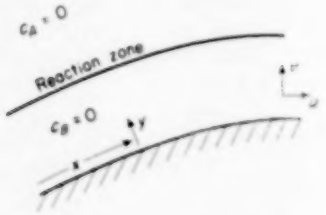

Fig. 1. A schematic diagram of the physical set-up.

In order now to achieve our main objective, which is to ascertain the effect of the chemical reaction on the rate of mass transfer of substance A, we shall limit ourselves to a hydrodynamic system, the laminar boundary layer flow, which has the unique property of being well enough defined to admit of a theoretical treatment, while at the same time being realized often enough in practice to be of more than academic interest.

Basic Equations and Their Solution

The process under consideration is governed by the diffusion equations for convective mass transfer of the two species A and B which, for laminar boundary layer flows, become [5, 6]

$$u_1 \frac{\partial c_A}{\partial x_1} + v_1 \frac{\partial c_A}{\partial y_1} = \frac{1}{Sc_A} \frac{\partial^2 c_A}{\partial y_1^2} \tag{1}$$

and

$$u_1 \frac{\partial c_B}{\partial x_1} + v_1 \frac{\partial c_B}{\partial y_1} = \frac{1}{Sc_B} \frac{\partial^2 c_A}{\partial y_1} \tag{2}$$

with the boundary conditions:

$$\left.\begin{array}{ll} c_A = c_A(0) & \text{at } y_1 = 0 \\ c_A = 0 & \text{at } x_1 = 0 \\ c_A = 0 & \text{at } y_1 = y_R(x_1) \\ c_B = c_B(\infty) & \text{at } y_1 = \infty \\ c_B = c_B(\infty) & \text{at } x_1 = 0 \\ c_B = 0 & \text{at } x_1 = y_R(x_1) \end{array}\right\} \tag{3}$$

where $y_R(x_1)$ denotes the position of the reaction zone. In addition, if the chemical reaction takes place according to the stoichiometric equation

$$aA + bB \rightarrow \text{products} \tag{4}$$

it is clear that a material balance around the reaction zone will yield the last boundary condition,

$$\frac{a}{Sc_A}\left(\frac{\partial c_A}{\partial y_1}\right)_{y_1 = y_R} = -\frac{b}{Sc_B}\left(\frac{\partial c_B}{\partial y_1}\right)_{y_1 = y_R} \tag{5}$$

In what follows, we shall suppose that the two velocity components u_1 and v_1, to be substituted in equations (1) and (2), may be obtained from the solution of the well-known laminar boundary layer equations for the transfer of momentum [6, 7]. It is realized of course that it is not quite correct, strictly speaking, to assume that the hydrodynamic equations may be solved independently from the mass transfer equations, for not only are the fluid properties in general dependent on composition but, as a direct consequence of the transfer of material at the surface, the normal component of the interfacial velocity is no longer zero. It is known, however, that the effects just mentioned are usually of secondary importance only and will therefore be disregarded for the purposes of this study.

Now, Friedlander and Litt [5] have already shown that equations (1) and (2) may be solved analytically, by a similarity transformation, only for flows past a wedge-type surface, of which the flat plate is but a special case. It is the purpose of the present analysis to remove this restriction and to obtain a solution to such a physical system

which will apply to two-dimensional surfaces of arbitrary geometry. This will be accomplished in the following manner: It was noted some time ago by FAGE and FALKNER [8] and proved rigorously by MORGAN and WARNER [9] for the analogous heat transfer problem that when the Schmidt number Sc is large it is permissible to replace the exact velocity components u_1 and v_1 in the diffusion equation by their asymptotic form near the surface. Furthermore, it was established by LIGHTHILL [10] in an often quoted paper that this asymptotic development, which strictly speaking becomes exact only when $Sc \to \infty$, is usually of acceptable accuracy even if Sc is around unity. This means therefore that, since for most gases $Sc \simeq 1$ and for all liquids $Sc > 1$, we may confine our attention to the asymptotic solution of equations (1) and (2) when both $Sc_A \to \infty$ and $Sc_B \to \infty$. For, in view of LIGHTHILL's results, we should expect that any conclusions derived from such an asymptotic analysis of our problem would also apply to essentially all possible cases of practical interest.

Thus, when both $Sc_A \gg 1$ and $Sc_B \gg 1$, the physical process of mass transfer and chemical reaction will take place in a region very close to the surface in which u_1 and v_1 may be represented respectively by

$$\left.\begin{aligned} u_1 &= \beta(x_1)\, y_1 \\ \text{and} \qquad v_1 &= -\frac{y_1^2}{2}\frac{d\beta}{dx_1} \end{aligned}\right\} \tag{6}$$

The function $\beta(x_1)$ is proportional to the shear stress at the surface which is either known or may be calculated for a large number of geometries by standard methods [7, 11, 12]. It is possible to show now that equations (1), (2), (3), (5) and (6) can be solved analytically by a similarity transformation. Let

$$\frac{c_A}{c_A(0)} \equiv \theta_A(\eta); \quad \frac{c_B}{c_B(\infty)} \equiv \theta_B(\eta)$$

where

$$\eta \equiv y_1 (Sc_A)^{1/3} \frac{\sqrt{\beta}}{\left[9^{1/3}\int_0^{x_1}\sqrt{\beta}\,dx\right]^{1/3}} \tag{7}$$

which reduces our system of equations to

$$\left.\begin{aligned} &\theta''_A + 3\eta^2\,\theta'_A = 0 \\ \text{and} \qquad &\theta''_B + 3\alpha\eta^2\,\theta'_B = 0 \end{aligned}\right\} \tag{8}$$

with the boundary conditions:

$$\left.\begin{aligned} &\theta_A(0) = 1, \quad \theta_A(\eta_R) = 0 \\ &\theta_B(\eta_R) = 0, \quad \theta_B(\infty) = 1 \\ \text{and} \qquad &\theta'_A(\eta_R) = -\lambda\,\theta'_B(\eta_R) \end{aligned}\right\} \tag{9}$$

η_R denotes the position of the reaction zone, defined by equation (7) with $y_1 \equiv y_R(x_1)$, and α and λ are two known fluid parameters given by

$$\alpha \equiv \frac{Sc_B}{Sc_A} \text{ and } \lambda \equiv \frac{a}{b}\frac{Sc_A}{Sc_B}\frac{c_B(\infty)}{c_A(0)}$$

Equations (8) and (9) may now be solved by elementary means. Thus

$$\theta_A = 1 - \frac{\int_0^{\eta^3} z^{-2/3}\exp(-z)\,dz}{\int_0^{\eta_R^3} z^{-2/3}\exp(-z)\,dz} \quad \text{for } 0 \leqslant \eta \leqslant \eta_R \tag{10}$$

and

$$\theta_B = \frac{\int_{\alpha\eta_R^3}^{\alpha\eta^3} z^{-2/3}\exp(-z)\,dz}{\int_{\alpha\eta_R^3}^{\infty} z^{-2/3}\exp(-z)\,dz} \quad \text{for } \eta_R \leqslant \eta \leqslant \infty \tag{11}$$

where η_R, which is a function only of λ and α, must be obtained from

$$\lambda\alpha^{1/3} = \exp\left[(\alpha-1)\,\eta_R^3\right]\frac{\int_{\alpha\eta_R^3}^{\infty} z^{-2/3}\exp(-z)\,dz}{\int_0^{\eta_R^3} z^{-2/3}\exp(-z)\,dz} \tag{12}$$

Since the integrals appearing in equations (10), (11) and (12) are expressible in terms of the incomplete gamma-function, already tabulated by PEARSON [13], the numerical evaluation of η_R, θ_A and θ_B can be performed quite readily. Of

particular interest is the rate is mass transfer of A. If

$$\mathrm{Nu} \equiv -L\left(\frac{\partial \theta_A}{\partial y}\right)_{y=0}$$

then, in view of equations (7) and (10)

$$\frac{\mathrm{Nu}}{\mathrm{Nu}_0} = \frac{\Gamma(1/3)}{\int_0^{\eta_R^3} z^{-2/3}\exp(-z)\,dz} \tag{13}$$

where Nu_0 is the Nusselt number in the absence of any chemical reaction ($\lambda = 0$ or $\eta_R \to \infty$) and is equal to

$$\mathrm{Nu}_0 = \sqrt{\mathrm{Re}}\left(\frac{\mathrm{Sc}_A}{9}\right)^{1/3} \frac{\sqrt{\beta}}{\Gamma(4/3)\left(\int_0^{x_1}\sqrt{\beta}\,dx\right)^{1/3}} \tag{14}$$

which is incidentally identical to the well-known Lighthill formula [10] for the analogous heat transfer problem.

The principal result of our analysis may now easily be deduced from equation (13), for it is clear that, since η_R according to equation (12) is determined solely by the numerical values of α and λ, the effect of the chemical reaction on the rate of mass transfer of A can be represented by a simple expression of the form

$$\mathrm{Nu} = C\,\mathrm{Nu}_0 \tag{15}$$

where the correction factor C which may be evaluated exactly from equations (12) and (13) is of a function only of the two dimensionless groups α and λ and is completely independent of the surface geometry. We have succeeded in establishing, therefore, that equation (15) which had already obtained by Friedlander and Litt [5] for the flat plate only, is valid for any two-dimensional surface.

Before concluding this section we shall briefly derive some useful properties of the function $C(\alpha, \lambda)$.

(1) A closed-form expression for $C(\alpha, \lambda)$ may easily be obtained when $\alpha = 1$, that is, where $\mathrm{Sc}_A = \mathrm{Sc}_B$. Thus it is obvious from equations (12) and (13) that under this condition

$$C(\alpha, \lambda) = 1 + \lambda$$

which, as can be verified from the basic differential equations themselves, is valid even where $\mathrm{Sc}_A < 1$.

(2) When $\lambda \to \infty$ one would certainly expect that the rate of mass transfer of A from the surface would be completely controlled by the rate of transfer of B from the bulk to the reaction zone. This is borne out by our results. Thus, as $\lambda \to \infty$, $\eta_R \to 0$ and therefore

$$C(\alpha, \lambda) \to \lambda\alpha^{1/3} \text{ as } \lambda \to \infty \tag{16}$$

The general behaviour of the function $C(\alpha, \lambda)$ between its two asymptotes, 1 and $\lambda\alpha^{1/3}$, is depicted in Fig. 2 for $\alpha = 10$, 1 and 0·1, while η_R, the predicted position of the reaction zone, is shown in Fig. 3.

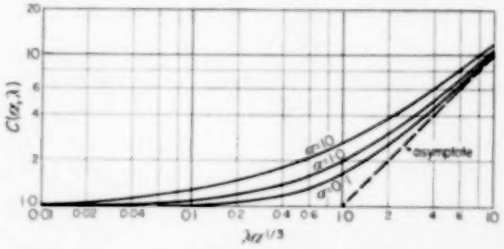

Fig. 2. The general behaviour of the function $C(\alpha, \lambda)$.

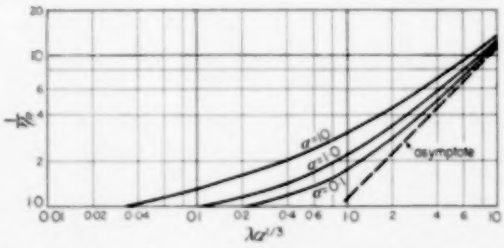

Fig. 3. The position of the reaction zone as a function of the two fluid parameters α and λ.

The Solution of the Energy Equation

Our general analysis can finally be extended to non-isothermal processes and may be used to predict the temperature rise in the reaction zone. This information is usually of some importance whenever chemical reactions take place and where large heat effects must be avoided.

VOL. 13 1961

For two-dimensional laminar boundary layer flows the temperature distribution is governed by the energy equation [6, 7]

$$u_1 \frac{\partial T}{\partial x_1} + v_1 \frac{\partial T}{\partial y_1} = \frac{1}{\mathrm{Pr}} \frac{\partial^2 T}{\partial y_1^2} \tag{17}$$

If again we make use of our asymptotic development with $\mathrm{Sc}_A \gg 1$ and $\mathrm{Sc}_B \gg 1$, we may replace u_1 and v_1 by equation (6) since the chemical reaction will occur in a region very close to the surface. Furthermore, if we let

$$T = T(\eta)$$

where, as before, η is given by equation (7), we can shown that

$$\frac{d^2T}{d\eta^2} + 3\alpha_1 \eta^2 \frac{dT}{d\eta} = 0 \tag{18}$$

where $\alpha_1 \equiv \dfrac{\mathrm{Pr}}{\mathrm{Sc}_A}$.

We shall now solve equation (18) subject to the boundary conditions:

(a) $T = T_\infty$ at $\eta = 0$ and $\eta = \infty$

(b) $$-\frac{\Delta H_R}{\rho C_p} \frac{\mathrm{Pr}}{\mathrm{Sc}_A} C_A(0) \left(\frac{d\theta_A}{d\eta}\right)_{\eta=\eta_R} = \left[\left(\frac{dT}{d\eta}\right)_{\eta=\eta_R+0} - \left(\frac{dT}{d\eta}\right)_{\eta=\eta_R-0}\right] \tag{19}$$

which is obtained from a heat balance around the reaction zone. Thus, if $\lambda_1 \equiv \dfrac{\Delta H_R}{\rho C_p} \dfrac{\mathrm{Pr}}{\mathrm{Sc}_A} c_A(0)$, we can readily verify that

(a) For $\eta \leqslant \eta_R$

$$\frac{T - T_\infty}{\lambda_1} = \frac{\exp(\alpha_1 - 1)\eta_R}{\alpha_1^{1/3}\Gamma(1/3)} \frac{\displaystyle\int_{\alpha_1\eta'_R}^{\infty} z^{-2/3}\exp(-z)\,dz}{\displaystyle\int_0^{\eta'_R} x^{-2/3}\exp(-z)\,dz} \int_0^{\alpha_1\eta'} z^{-2/3}\exp(-z)\,dz \tag{20}$$

(b) For $\eta \geqslant \eta_R$

$$\frac{T - T_\infty}{\lambda_1} = \frac{\exp(\alpha_1 - 1)\eta_R}{\alpha_1^{1/3}\Gamma(1/3)} \int_0^{\alpha_1\eta_R} z^{-2/3}\exp(-z)\,dz \Bigg/ \int_0^{\eta'_R} z^{-2/3}\exp(-z)\,dz \int_{\alpha_1\eta'_R}^{\infty} z^{-2/3}\exp(-z)\,dz \tag{20a}$$

Of particular interest is the maximum value of the temperature, T_m, which is obtained from equation (20) by letting $\eta = \eta_R$. Under special conditions two simple expressions can be derived:

(a) When $\alpha_1 = 1$, which is usually obeyed approximately by most gases,

$$\frac{T_m - T_\infty}{\lambda} = \frac{C - 1}{C} \tag{21}$$

where C is given by equations (13) and (15).

(b) When $\lambda \to \infty$, that is, when the process is controlled by the rate of transfer of B from the bulk to the reaction zone,

$$\frac{T_m - T_\infty}{\lambda_1} = 1 \tag{22}$$

It is, moreover, easy to show, from an analysis of the basic differential equations, that this is a more general result which is not restricted to the simple system considered in this work.

Conclusions

In this paper we have presented a theoretical analysis of a mass transfer process which is coupled with an instantaneous homogeneous chemical reaction between two substances. We have shown how it is possible to obtain a closed-form solution to the appropriate equations of diffusion and energy in laminar boundary layer flows past two-dimensional surfaces of arbitrary geometry, by making use of an asymptotic development which, although strictly speaking exact only when the Schmidt numbers of both diffusing species approach infinity, is of acceptable accuracy even when $\mathrm{Sc} \sim 1$. As a consequence the results of our present work should apply

to most physical systems of interest under laminar boundary layer flow conditions.

The principal conclusion of this analysis concerns the way in which the rate of mass transfer of one of the reacting species from the surface is influenced by the presence of the chemical reaction. We have been able to show that, if Nu is the local Nusselt number and Nu_0 the the Nusselt number in the absence of a chemical reaction, then

$$\mathrm{Nu} = \mathrm{Nu}_0\, C(\alpha, \lambda)$$

where the correction factor $C(\alpha, \lambda)$, which may be evaluated exactly from equations (12) and (13), is a function only of the two fluid parameters α and λ, and is independent of the surface geometry.

Acknowledgements—This work was supported in part by a grant from the National Science Foundation.

NOTATION

a, b = stoichiometric coefficients of the chemical reaction
A, B = the two reacting components A and B
C_p = specific heat
C_A = concentration of component A
$c_A(0)$ = concentration of A in the fluid next to the surface
c_B = concentration of component B
$c_B(\infty)$ = concentration of B in the bulk
$C(\alpha, \lambda)$ = a function defined by equations (13) and (15)
D = diffusion coefficient
k = thermal conductivity
L = characteristic length
T = temperature of the fluid
T_∞ = temperature in the bulk of the fluid
U_∞ = characteristic velocity of the stream
u = x-component of the velocity ($u_1 = u/U_\infty$)
v = y-component of the velocity ($v_1 = \sqrt{\mathrm{Re}}\, v/U_\infty$)
x = distance along the surface from the leading edge $x_1 = (x/L)$
y = distance normal to the surface ($y_1 = \sqrt{\mathrm{Re}}\, y/L$)
$y_R(x_1)$ = the distance of the reaction zone from the surface
α = dimensionless fluid parameter defined by $\alpha = \mathrm{Sc}_B/\mathrm{Sc}_A$
α_1 = dimensionless fluid parameter defined by $a_1 = \mathrm{Pr}/\mathrm{Sc}_A$
$\beta(x_1) = \dfrac{1}{\sqrt{\mathrm{Re}}} \dfrac{\tau_0 L}{\mu U_\infty}$
θ_A = dimensionless concentration $\theta_A = c_A/c_A(0)$
θ_B = dimensionless concentration $\theta_B = c_B/c_B(\infty)$
η = similarity variable defined by equation (7)
η_R = the position of the reaction zone [defined by equation (7) with $y_1 = y_R(x_1)$]
λ = dimensionless fluid parameter;
$$\lambda = \frac{a}{b} \frac{\mathrm{Sc}_A}{\mathrm{Sc}_B} \frac{c_B(\infty)}{c_A(0)}$$
λ_1 = fluid parameter with units of temperature;
$$\lambda_1 = \frac{\Delta H_R}{\rho C_p} \frac{\mathrm{Pr}}{\mathrm{Sc}_A} c_A(0)$$
μ = viscosity
ν = kinematic viscosity
ρ = mass density
τ_0 = local shear stress at the surface
ΔH_R = the heat of reaction per unit mole ($\Delta H_R > 0$ for an exothermic reaction)
Nu = the local Nusselt for the transfer of A; $\mathrm{Nu} = -L(\partial\theta_A/\partial y)_{y=0}$
Nu_0 = the local Nusselt number in the absence of a reaction ($\lambda = 0$)
Re = $U_\infty L/\nu$, the Reynolds number
Pr = $C_p \mu/k$, the Prandtl number
Sc = ν/D, the Schmidt number

REFERENCES

[1] CHAMBRÉ P. L. and ACRIVOS A. *J. Appl. Phys* 1956 **27** 1322; *Industr. Engng. Chem.* 1957 **49** 1025.
[2] CHAMBRÉ P. L. *Appl. Sci. Res. Hague.* 1956 A **6** 97; *Phys. Fluids* 1958 **1** 48.
[3] KATZ S. *Chem. Engng. Sci.* 1959 **10** 202.
[4] ROSNER D. E. *Jet Propulsion* 1958 **28** 445.
[5] FRIEDLANDER S. K. and LITT M. *Chem. Engng. Sci.* 1958 **8** 229
[6] PAI S. I. *Viscous Flow Theory* Vol. I. Van Nostrand, New York 1956.
[7] SCHLICHTING H. *Boundary Layer Theory* McGraw-Hill, New York 1955.
[8] FAGE A. and FALKNER V. M. Aeronautical Research Committee, London. Report and Memorandum No. 1408 (1931).
[9] MORGAN G. W. and WARNER W. H. *J. Aero. Sci.* 1956 **23** 937.
[10] LIGHTHILL M. J. *Proc. Roy. Soc. Lond.* 1950 A **202** 369.
[11] ACRIVOS A. *J. Aero. Space Sci.* 1960 **27** 314.
[12] GÖRTLER H. *J. Math. and Mech.* 1957 **6** 1.
[13] PEARSON K. *Tables of the Incomplete Γ-Function* 1922.

Chemical Engineering Science, 1960, Vol. 13, pp. 63 to 68. Pergamon Press Ltd., London. Printed in Breat Gritain

Axial diffusion in isothermal tubular flow reactors

LIANG-TSENG FAN and RICHARD C. BAILIE
Kansas State University of Agriculture and Applied Science,
Manhattan, Kansas, U.S.A.

(*Received* 28 *January* 1960; *in revised form* 10 *May* 1960)

Abstract—Numerical solutions are presented for differential equations representing the isothermal steady flow tubular reactors with varied degrees of backmixing of the reactants in the axial direction and with reactions with order other than zero and first.

Résumé—Les auteurs présentent des solutions numériques pour les équations différentielles représentant l'écoulement stationnaire isotherme dans des réacteurs tubulaires présentant des degrés divers de mélange en retour des réactifs dans le sens axial et pour des réactions dont l'ordre est différent de zéro ou de un.

Zusammenfassung—Es werden numerische Lösungen von Differentialgleichungen für isotherme kontinuierliche Rohrreaktoren angegeben, wobei eine verschieden starke Rückvermischung der Reaktanden in axialer Richtung berücksichtigt wird. Diese Lösungen gelten für alle Reaktionsordnungen ausser der nullten und der ersten.

INTRODUCTION

A MATERIAL balance in a tubular flow reactor operated under isothermal steady state conditions yields the following equation:

$$\bar{E}\frac{d^2C}{dz^2} - \bar{u}\frac{dC}{dz} - r(c) = 0 \qquad (1)$$

When the reaction is of n-th order involving one reactant or several reactants with equivalent concentration, the rate of reaction $r(c)$ is represented as:

$$r = kC^n$$

The boundary conditions are as follows [1]:

$$z = 0, \quad \frac{dC}{dz} = \frac{\bar{u}}{\bar{E}}(C_0 - C_{z\to 0}) \qquad (2)$$

$$z = L, \quad \frac{dC}{dz} = 0$$

The following transformations of the variables lead to the dimensionless form of differential equation which contains two parameters; one, U, being associated with the ratio of flow and diffusion velocities and the other, R_n, with the ratio of reaction and flow velocities.

$$Y = \frac{C}{C_0}, \quad \frac{z}{L} = \eta$$

$$\frac{d^2Y}{d\eta^2} - 2U\frac{dY}{d\eta} - UR_n Y^n = 0 \qquad (3)$$

where $U = \dfrac{\bar{u}L}{2\bar{E}}$ and $R_n = \dfrac{2k_nL}{\bar{u}}C_0^{n-1}$

The boundary conditions are transformed to

$$\eta = 0, \quad \frac{dY}{d\eta} = 2U(Y_{\eta\to 0+} - 1)$$

$$\eta = 1, \quad \frac{dY}{d\eta} = 0 \qquad (4)$$

For the zero and the first-order reactions equation (3) yields linear ordinary differential equations and analytical solutions are available for them [1, 2].

For chemical reactions other than zero and first order equation (3) yields non-linear second-order ordinary differential equations. Anayltical solutions for them are not available. Because of their importance for reactor design numerical solutions were attempted by the authors.

NUMERICAL SOLUTION

The truncated finite-difference representation of the differential equation given by equation (3) yields [3]

$$Y_{i-1}(1 + Uh) + Y_{i+1}(1 - Uh) - 2Y_i - UR_n Y_i^n h^2 = 0 \qquad (5)$$

where h is the constant interval between pivotal points and i refers to i-th pivotal points.

The boundary conditions given by equation (4) may be represented as [3]

$$\eta = 1, \quad Y_p = Y_{p+1} \qquad (6)$$

$$\eta = 0, \quad Y_1 - Y_{-1} - 4hUY_0 + 4hU = 0 \qquad (7)$$

where p is the number of pivotal points.

Several criteria were used to insure the precision of the numerical solution to the finite difference equation. Only slight improvement in precision was obtained by increasing the number of increments used in the solution of the finite equation when the number of increments exceeded fifty. The boundary condition at $\eta = 1$ as represented by equation (6) was used as the starting point in the solution of the finite difference equation. The values of Y at the pivotal points were then obtained by means of equation (5). The boundary condition at $\eta = 0$, represented by equation (7), was used to check the calculation. An assumed value of Y at $\eta = 1$ was systematically changed by incremental values and the residue of equation (7) computed. The assumed value of Y leading to the smallest residue gives the closest solution to the differential equation. Smaller increments of Y at $\eta = 1$ insure residues approaching zero, i.e. greater precision. In the data presented here the final increment used was 0·1 per cent of the value of Y at $\eta = 1{\cdot}0$, and the number of pivotal points used set at 50. Further increase in precision could be obtained but would not alter the curves presented here.

Results and Discussion

Results of the numerical computations described in the previous section are plotted in Figs. 1–14 for $\frac{1}{4}$-, $\frac{1}{2}$-, second- and third-order reactions. (Similar diagrams for any combination of n, R_n and U may be obtained from the authors). Computations have been made for the case of second-order reactions by LEVENSPIEL and BISCHOFF [4]. The effect of axial diffusion on the concentration profile and degree of conversion of reactant is clearly illustrated in those figures.

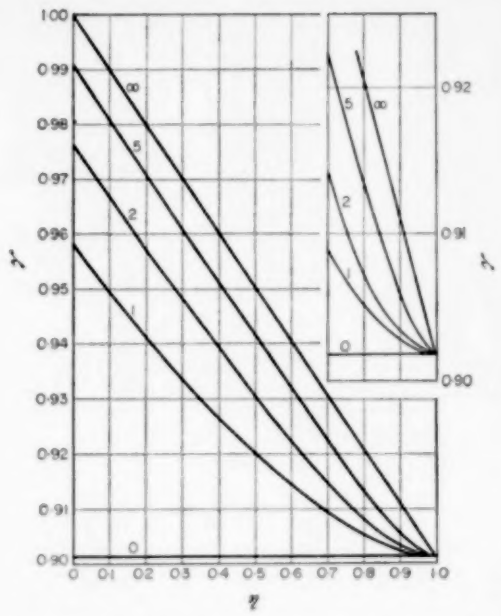

FIG. 1. Concentration profile of reactant in reactor for $\frac{1}{4}$-order reaction when $R_n = 0{\cdot}2$ $n = \frac{1}{4}$ $R_n = 0{\cdot}2$ v = Parameter.

The figures also show that the backmixing has profound effect on the concentration profile in the reactor in all the cases. It has, however, little or negligible effect on over-all conversion when the order of reactions is small, (theoretically it has no effect for zero-order reaction) especially when R_n is small.

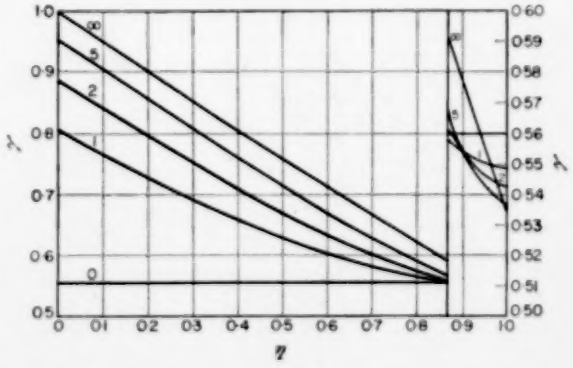

FIG. 2. Concentration profile of reactant in reactor for $\frac{1}{4}$-order reaction where $R_n = 1$ $n = \frac{1}{4}$ $R_n = 1$ v = Parameter.

VOL. 13 1961

When the axial diffusion of reactant is negligible equation (3) reduces to:

$$-\frac{dY}{d\eta} = \frac{R_n}{2} Y^n \tag{8}$$

Consequently, for n other than 1:

$$Y = \left[1 - \frac{R_n (1-n)}{2} \eta\right]^{1/(1-n)} \tag{9}$$

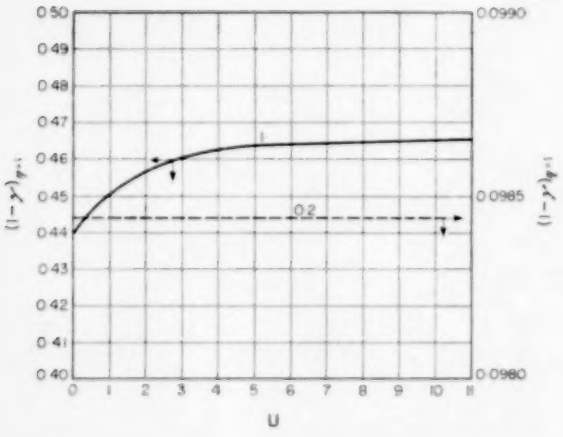

Fig. 3. Over-all conversion as a fraction of reactant fed for ½-order reaction, $n = \frac{1}{2}$ R_n = Parameter.

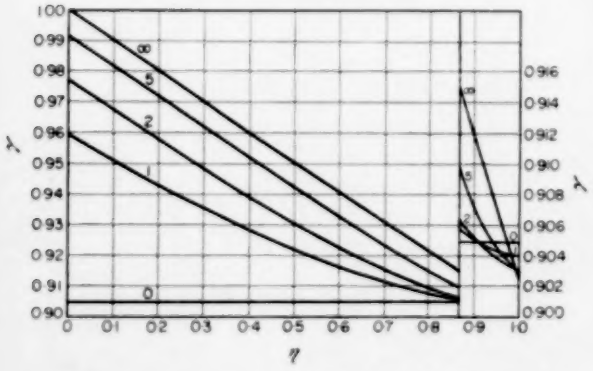

Fig. 4. Concentration profile of reactant in reactor for ½-order reaction when $R_n = 0{\cdot}2$ $n = \frac{1}{2}$ v = Parameter.

When the axial diffusion is infinitely large and the concentration of the reactant is uniform in the reactors:

$$\frac{R_n}{2} Y^n + Y - 1 = 0 \tag{10}$$

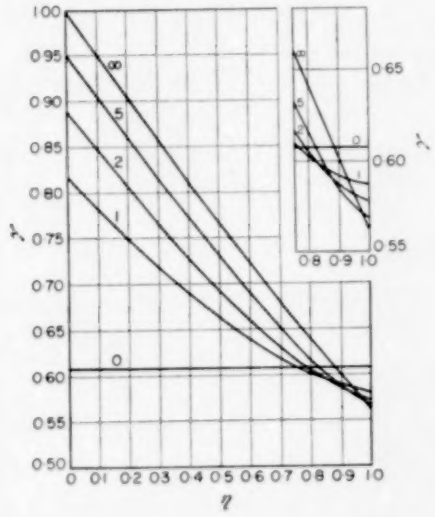

Fig. 5. Concentration profile of reactant in reactor for ½-order reaction when $R_n = 1$ $n = \frac{1}{2}$ v = Parameter.

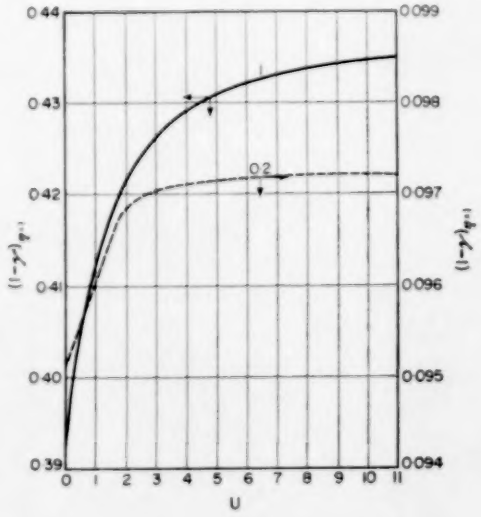

Fig. 6. Over-all conversion as a fraction of reactant fed for ½-order reaction $n = \frac{1}{2}$ R_n = Parameter.

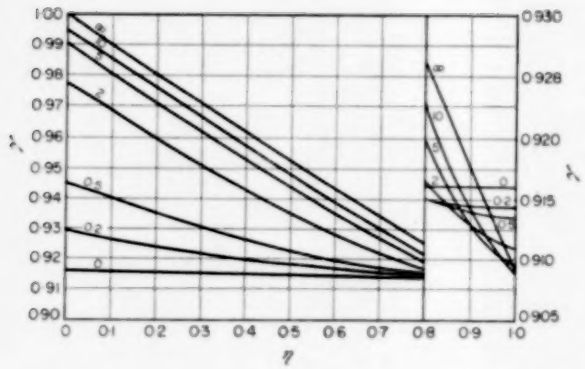

FIG. 7. Concentration profile of reactant in reactor for second-order reaction when $R_n = 0{\cdot}2$ $n = 2$ v = Parameter.

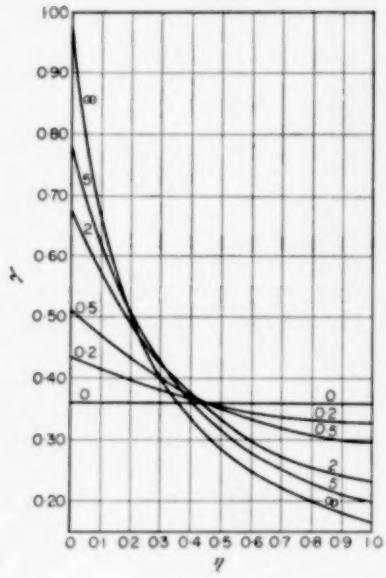

FIG. 9. Concentration profile of reactant in reactor for second-order reaction when $R_n = 10$ $n = 2$ v = Parameter.

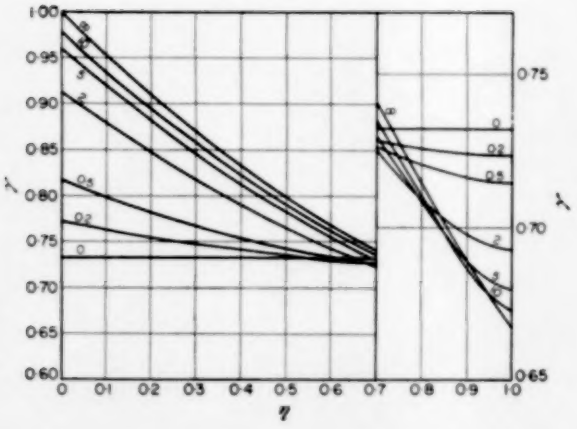

FIG. 8. Concentration profile of reactant in reactor for second-order reaction when $R_n = 1$ $n = 2$ v = Parameter.

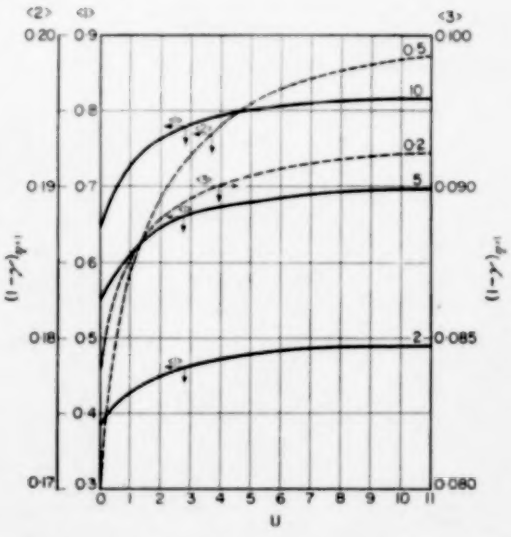

FIG. 10. Over-all conversion as a fraction of reactant fed second-order reaction. $n = 2$ R_n = Parameter.

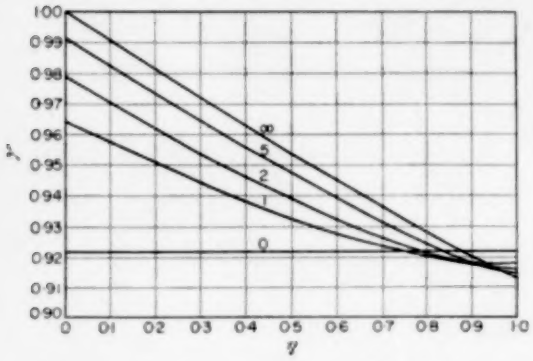

FIG. 11. Concentration profile of reactant in reactor for this order reaction when $R_n = 0{\cdot}2$ $n = 3$ v = Parameter.

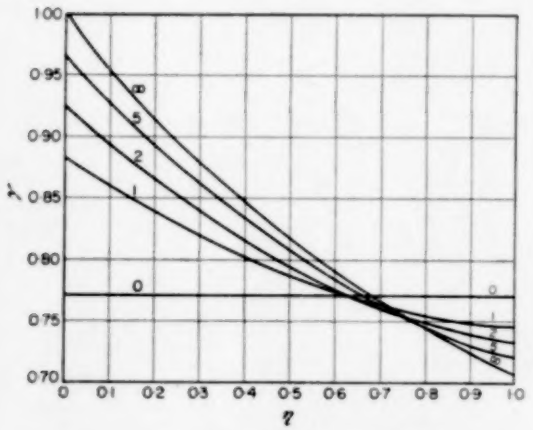

FIG. 12. Concentration profile of reactant in reactor for this order reaction when $R_n = 1$ $n = 3$ v = Parameter.

Equations (9) and (10) were used as criteria for validity of the numerical analysis employed. By increasing the values of U the concentration profile approaches asymptotically to that represented by equation (9), while by reducing the values of U it approaches the concentration profile represented by equation (10).

The results of this work show that the extrapolation or interpolation of concentration profile for the various order of reactions with the various degrees of backmixing is difficult. Therefore separate numerical solutions as illustrated in this article would be necessary for each different condition of reactor operation.

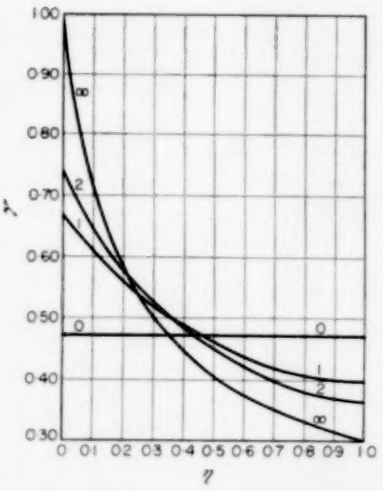

FIG. 13. Concentration profile of reactant in reactor for third-order reaction when $R_n = 10$ $n = 2$ v = Parameter.

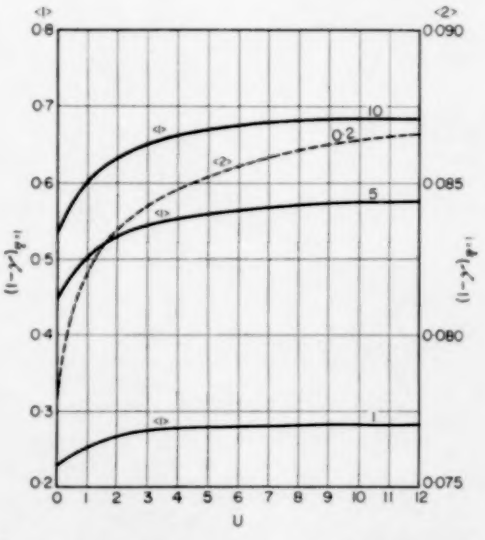

FIG. 14. Over-all conversion as a fraction of reactant fed third-order reaction. $n = 3$ R_n = Parameter.

NOTATION

C = concentration of reactant
C_0 = inlet concentration of reactant
E = axial diffusivity of reactant
$\bar{E}$ = mean value of E
h = constant interval
k_n = rate constant of n-th order reaction
L = length of reactor
n = order of reaction
P = number of pivotal points in finite difference calculation
$R_n = \dfrac{2 k_n L}{\bar{u}} C_0^{n-1}$
$\bar{u}$ = mean linear velocity of reacting mixture
$U = \dfrac{\bar{u} L}{2 E}$
z = co-ordinate in the direction of flow
$\eta = \dfrac{z}{L}$, dimensionless distance from inlet of reactor
$Y = \dfrac{C}{C_0}$, dimensionless concentration

REFERENCES

[1] DANCKWERTS P. V. *Chem. Engng. Sci.* 1953 **2** 1.

[2] YAGI S. and MIYAUCHI T. *Chem. Engng.* (*Japan*) 1955 **19** 507.

[3] FOX L. *Numerical Solution of Two-Point Boundary Problems in Ordinary Differential Equation.* Oxford University Press, 1957.

[4] LEVENSPIEL O. and BISCHOFF K. B. *Industr. Engng. Chem.* 1959 **51** 1431.

VOL
13
1961

Chemical Engineering Science, 1960, Vol. 13, pp. 69 to 74. Pergamon Press Ltd., London. Printed in Great Britain

Zur Messung der transversalen effektiven Diffusion in durchströmten Füllkörpersäulen

J. W. HIBY und P. SCHÜMMER
Forschungsinstitut Verfahrenstechnik der GVT, Aachen, Germany

(*Received* 30 *January* 1960)

Zusammenfassung—Für die Messung der effektiven Diffusion und effektiven Wärmeleitung in radialer Richtung in einem festen oder fluidisierten Bett ist eine Anordnung geeignet, bei der der radiale Austausch zwischen zwei konzentrischen Bereichen der Strömung erfolgt. Die für die Auswertung erforderliche Integration der Differentialgleichung wird durchgeführt unter Berücksichtigung von Wandreflexion und longitudinaler Diffusion. Die numerische Ermittlung der Lösung bezieht sich auf einen Bereich, in dem die longitudinale Diffusion vernachlässigt werden darf.

Abstract—Effective diffusion as well as effective thermal conductivity in transverse direction in a fixed or fluidized bed can be measured in a column where radial exchange takes place between two concentric areas of the flow field. In this article an integration of the underlying differential equation is given, allowing for reflexion at the tube wall and for longitudinal diffusion. The solution is evaluated numerically for a range of conditions where longitudinal diffusion may be neglected.

Résumé—On peut mesurer la diffusion effective et la conductivité thermique effective dans le sens transversal d'un lit fixe ou turbulent, dans une colonne lorsque l'échange radial s'effectue entre deux zones concentriques du champ d'écoulement. L'article fournit une intégration de l'équation différentielle, permettant de tenir compte de la reflection sur la paroi et de la diffusion longitudinale. La solution numérique est évaluée numériquement pour un intervalle de conditions lorsque la diffusion longitudinale peut être négligée.

ZUR Messung der diffusionsartigen Querausbreitung (transversale effektive Diffusion) in Füllkörpersäulen oder verwandten Medien leitet man gewöhnlich einen geeigneten Indikator zentrisch und kontinuierlich in die Strömung ein. Zur einfachen Auswertung wird die Quelle als punktförmig angenommen. Aus der Konzentrationsverteilung in einem stromabwärts gelegenen Querschnitt gewinnt man die modellmässige Kenngrösse für die Querausbreitung. Hierbei kann mit Hilfe einer Lösung von KLINKENBERG, KRAJENBRINK und LAUWERIER [1] auch der Einfluss einer Längsausbreitung berücksichtigt werden.

Bei einer Untersuchung über Querausbreitung, über die an anderer Stelle berichtet wird [2], haben wir andere Randbedingungen gewählt. Die indizierte Flüssigkeit wird durch eine Röhre

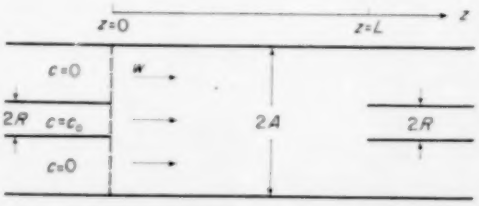

ABB. 1. Schematischer Längsschnitt durch die mit Füllkörpern gefüllte Säule.

(Durchmesser $2R$) zentrisch zur Hauptströmung (Säulendurchmesser $2A$) eingeleitet (Abb. 1). Die Strömungsgeschwindigkeit w ist in beiden konzentrischen Bereichen über die gesamte Säulenlänge gleich. Im Abstand L von der Aufgabestelle wird durch ein ebenfalls zentrisches Rohr gleichen Durchmessers $2R$ die Messflüs-

sigkeit entnommen und aus ihrem mittleren Gehalt an Indikator die Kenngrösse der Querausbreitung berechnet. Diese Methode vermeidet die mit der Realisierung einer Punktquelle verbundenen Schwierigkeiten; ein weiterer Vorteil ist die Mittelung über alle Azimutrichtungen und die Entnahme der Messflüssigkeit im Innern der nahezu ungestörten Packung. Die genannten Randbedingungen eignen sich nicht nur zur Messung der effektiven Diffusion in Festbetten und fluidisierten Betten, sondern auch zur Messung der effektiven Wärmeleitfähigkeit. Wir möchten deshalb die zur Auswertung erforderliche Rechnung und ihre Ableitung hier gesondert mitteilen.

Wir bezeichnen die Koeffizienten der diffusionsartigen Ausbreitung (Mischungskoeffizienten) mit M_{tr} und M_l. Da die Ausbreitung im allgemeinen nicht isotrop erfolgt, wird zwischen dem transversalen und dem longitudinalen Mischungskoeffizienten unterschieden. Die Längsausbreitung ist jedoch in manchen Fällen wegen des geringen Konzentrationsgradienten in Achsenrichtung zu vernachlässigen. Wann dies erlaubt ist, muss eine Überschlagsrechnung zeigen, die an der Funktion für die Konzentrationsverteilung durchzuführen ist (Gleichung 3).

Aus dem Elementargesetz der anisotropen diffusiven Ausbreitung, $\mathbf{j} = -\mathbf{M}\cdot\nabla c + c\,\mathbf{v}$, wobei $\mathbf{M}$ ein Tensor (zweiter Stufe) mit der Matrix

$$\begin{pmatrix} M_z & 0 & 0 \\ 0 & M_r & 0 \\ 0 & 0 & M_\phi \end{pmatrix}$$

ist, folgt als Kontinuitätsgleichung für den sich einstellenden stationären Zustand die Differentialgleichung

$$\frac{\partial^2 c}{\partial r^2} + \frac{1}{r}\frac{\partial c}{\partial r} + \frac{M_l}{M_{tr}}\frac{\partial^2 c}{\partial z^2} - \frac{w}{M_{tr}}\frac{\partial c}{\partial z} = 0.$$

(Vergl. die Erklärung der Zeichen am Schluss der Arbeit).

Es wurde $M_z = M_l$ und $M_r = M_\phi = M_{tr}$ angenommen.

Als Randwertbedingungen werden eingeführt:

$$r = A: \qquad \frac{\partial c}{\partial r} = 0 \text{ (Wandreflexion)}$$

$$z = 0: \qquad r < R: \quad wc_0 = wc - M_l\frac{\partial c}{\partial z},$$

$$R < r < A: \quad 0 = wc - M_l\frac{\partial c}{\partial z},$$

d.h. die Einlassebene wird als undurchlässig gegenüber diffusiver Rückmischung angenommen. In der Messebene ($z = L$) sei der mit der z-Richtung abnehmende axiale Konzentrationsgradient schon so klein, dass ein Einfluss des Säulenauslaufs infolge diffusiver Rückmischung zur Messebene vernachlässigt werden kann; die Säule wird also in Strömungsrichtung als unendlich angenommen.

Nach Einführung dimensionsloser Grössen*

$$y = \frac{c}{c_0},\ \rho = \frac{r}{A},\ \zeta = \frac{z}{d},\ \mathrm{Bo}_l = \frac{dw}{M_l},\ \mathrm{Bo}_{tr} = \frac{dw}{M_{tr}},\ k = \frac{A}{d}$$

in denen d eine für die Packung charakteristische Länge, z.B. Teilchengrösse, ist, lauten die Differentialgleichung und ihre Randbedingungen:

$$\frac{\partial^2 y}{\partial \rho^2} + \frac{1}{\rho}\frac{\partial y}{\partial \rho} + k^2\frac{\mathrm{Bo}_{tr}}{\mathrm{Bo}_l}\frac{\partial^2 y}{\partial \zeta^2} - \mathrm{Bo}_{tr}k^2\frac{\partial y}{\partial \zeta} = 0 \quad (1)$$

$$\rho = 1: \qquad \frac{\partial y}{\partial \rho} = 0 \quad (2a)$$

$$\left.\begin{array}{l} \zeta = 0: \quad 0 < \rho < \dfrac{R}{A}: f(\rho) \equiv y - \dfrac{1}{\mathrm{Bo}_l}\dfrac{\partial y}{\partial \zeta} = 1 \\ \qquad\quad \dfrac{R}{A} < \rho < 1: f(\rho) \equiv y - \dfrac{1}{\mathrm{Bo}_l}\dfrac{\partial y}{\partial \zeta} = 0 \end{array}\right\} \quad (2b)$$

Ein Ansatz der Form $y = P(\rho)\cdot Z(\zeta)$ führt auf die verträgliche, überall endliche Partikularlösung:

$$y = C_\nu J_0(\rho\,\lambda_\nu)\exp\left\{-\zeta\,\mathrm{Bo}_l\left[\left(\tfrac{1}{4} + \frac{\lambda_\nu^2}{k^2\,\mathrm{Bo}\,\mathrm{Bo}_{trl}}\right)^{1/2} - \tfrac{1}{2}\right]\right\},$$

$J_0(\rho\,\lambda_\nu)$ = Besselfunktion der Ordnung Null.

*Auf Vorschlag von D. W. van Krevelen [3] wird die Kennzahl der diffusiven Ausbreitung nach Bodenstein benannt; sie entspricht der für Temperaturleitung definierten Péclet-zahl.

VOL. 13 1961

Die Lösung des Randwertproblems werde als eine Summation über solche Partikularlösungen angesetzt (Fouriersche Methode):

$$y = \sum_{(\nu)} C_\nu \, J_0(\rho \lambda_\nu) \exp\left\{ -\zeta \, \mathrm{Bo}_l \left[\left(\tfrac{1}{4} + \frac{\lambda_\nu^2}{k^2 \, \mathrm{Bo}_{tr} \, \mathrm{Bo}_l} \right)^{1/2} - \tfrac{1}{2} \right] \right\}.$$

Aus der Randbedingung

$$\frac{\partial y}{\partial \rho} = - \sum_{(\nu)} C_\nu \lambda_\nu \, J_1(\rho \lambda_\nu) \exp\left\{ -\zeta \, \mathrm{Bo}_l \left[\left(\tfrac{1}{4} + \frac{\lambda_\nu^2}{k^2 \, \mathrm{Bo}_{tr} \, \mathrm{Bo}_l} \right)^{1/2} - \tfrac{1}{2} \right] \right\} = 0$$

für $\rho = 1$

folgt $J_1(\lambda_\nu) = 0$.

Die Summation ist also über alle Wurzeln der Gleichung $J_1(\lambda) = 0$ zur erstrecken:

$$\lambda_0 = 0\,; \; \lambda_1 = 3{,}8317\,; \; \lambda_2 = 7{,}0156\,; \; \lambda_3 = 10{,}1735 \text{ u.s.f.}$$

Zur Bestimmung der C_ν benutzt man die Randbedingung der Gleichungen (2b). Die Funktionen $u_\nu = \rho^{1/2} J_0(\rho\lambda_\nu)$ mit $J_1(\lambda_\nu) = 0$ bilden einen vollständigen Satz von Orthogonalfunktionen. Die C_ν ergeben sich mit Hilfe der Orthogonaleigenschaft $\int_0^1 \rho \, u_\nu \, u_\mu \, d\rho = 0$, $(\nu \neq \mu)$. Es sei weiter μ ein beliebiger Wert unter den natürlichen Zahlen ν. Dann errechnet sich schrittweise (vgl. Definition von $f(\rho)$ in Gleichung (2b)):

$$f(\rho) = \sum_{(\nu)} C_\nu \left[\left(\tfrac{1}{4} + \frac{\lambda_\nu^2}{k^2 \, \mathrm{Bo}_{tr} \, \mathrm{Bo}_l} \right)^{1/2} + \tfrac{1}{2} \right] J_0(\rho \lambda_\nu),$$

$$f(\rho) \, \rho \, J_0(\rho \lambda_\mu) = \sum_{(\nu)} C_\nu \, \rho \, J_0(\rho \lambda_\nu) \, J_0(\rho \lambda_\mu) \times \left[\left(\tfrac{1}{4} + \frac{\lambda_\nu^2}{k^2 \, \mathrm{Bo}_{tr} \, \mathrm{Bo}_l} \right)^{1/2} + \tfrac{1}{2} \right].$$

$$\mu = \nu : \int_0^1 \rho f(\rho) \, J_0(\rho \lambda_\nu) \, d\rho = C_\nu \left[\left(\tfrac{1}{4} + \frac{\lambda_\nu^2}{k^2 \, \mathrm{Bo}_{tr} \, \mathrm{Bo}_l} \right)^{1/2} + \tfrac{1}{2} \right] \int_0^1 \rho \, J_0^2(\rho \lambda_\nu) \, d\rho.$$

$$C_\nu = \frac{2 J_1(\lambda_\nu R/A)}{\lambda_\nu \, J_0^2(\lambda_\nu)} \cdot \frac{R/A}{[\tfrac{1}{4} + (\lambda_\nu^2/k^2 \, \mathrm{Bo}_{tr} \, \mathrm{Bo}_l)]^{1/2} + \tfrac{1}{2}}.$$

Die Konzentrationsverteilung folgt somit der Funktion:

$$y = 2 \frac{R}{A} \sum_{\nu=0}^{\infty} \frac{J_1(\lambda_\nu R/A)}{\lambda_\nu \, J_0^2(\lambda_\nu)} \, J_0(\lambda_\nu \rho) \, \frac{\exp\left\{ -\zeta \, \mathrm{Bo}_l \left[[\tfrac{1}{4} + (\lambda_\nu^2/k^2 \, \mathrm{Bo}_{tr} \, \mathrm{Bo}_l)]^{1/2} - \tfrac{1}{2} \right] \right\}}{[\tfrac{1}{4} + (\lambda_\nu^2/k^2 \, \mathrm{Bo}_{tr} \, \mathrm{Bo}_l)]^{1/2} + \tfrac{1}{2}} \quad (3)$$

Für den Term $\nu = 0$ ist hier und in der Folge zu beachten, dass

$$J_0(0) = 1 \text{ und } \lim_{\lambda \to 0} \frac{J_1(\lambda)}{\lambda} = \tfrac{1}{2} \text{ gilt.}$$

Durch jeden Querschnitt der Säule muss wegen der Stationarität des Vorganges die gleiche Indikatormenge fliessen. Dass diese Bedingung erfüllt ist, zeigt eine Integration über den Flussvektor $j_z = wc - M_l \, \partial c/\partial z$:

$$Q = \int_{(F)} j_z \, dF = 2\pi \, A^2 \, w c_0 \int_0^1 \left(y - \frac{1}{\mathrm{Bo}_l} \frac{\partial y}{\partial \zeta} \right) \rho \, d\rho.$$

Es ist

$$\int_0^1 y \rho \, d\rho = 2 \frac{R}{A} \sum_{\nu=0}^{\infty} \frac{J_1(\lambda_\nu R/A)}{\lambda_\nu \, J_0^2(\lambda_\nu)} \times \frac{\exp\left\{ -\zeta \, \mathrm{Bo}_l \left[[\tfrac{1}{4} + (\lambda_\nu^2/k^2 \, \mathrm{Bo}_{tr} \, \mathrm{Bo}_l)]^{1/2} - \tfrac{1}{2} \right] \right\}}{[\tfrac{1}{4} + (\lambda_\nu^2/k^2 \, \mathrm{Bo}_{tr} \, \mathrm{Bo}_l)]^{1/2} + \tfrac{1}{2}} \times \int_0^1 J_0(\lambda_\nu \rho) \, \rho \, d\rho,$$

$$- \int_0^1 \frac{1}{\mathrm{Bo}_l} \frac{\partial y}{\partial \zeta} \rho \, d\rho = 2 \frac{R}{A} \sum_{\nu=0}^{\infty} \frac{J_1(\lambda_\nu R/A)}{\lambda_\nu \, J_0^2(\lambda_\nu)} \frac{\exp\left\{ -\zeta \, \mathrm{Bo}_l \left[[\tfrac{1}{4} + (\lambda_\nu^2/k^2 \, \mathrm{Bo}_{tr} \, \mathrm{Bo}_l)]^{1/2} - \tfrac{1}{2} \right] \right\}}{[\tfrac{1}{4} + (\lambda_\nu^2/k^2 \, \mathrm{Bo}_{tr} \, \mathrm{Bo}_l)]^{1/2} + \tfrac{1}{2}} \times \left[\left(\tfrac{1}{4} + \frac{\lambda_\nu^2}{k^2 \, \mathrm{Bo}_{tr} \, \mathrm{Bo}_l} \right)^{1/2} - \tfrac{1}{2} \right] \times \int_0^1 J_0(\lambda_\nu \rho) \, \rho \, d\rho.$$

Das Integral $\int_0^1 J_0(\lambda_\nu \rho) \, \rho \, d\rho$ nimmt für $\lambda_\nu \neq \lambda_0 = 0$ den Wert Null an wegen

$$\int_0^1 J_0(\lambda_\nu \rho)\, \rho\, d\rho = \frac{1}{\lambda_\nu^2} J_1(\lambda_\nu) = 0,\ \lambda_\nu \neq 0.$$

Im Fall $\lambda_\nu = \lambda_0 = 0$ folgt $\int_0^1 \rho\, d\rho = \frac{1}{2}$.

Die Integration über den konvektiven Transport ergibt also für sich allein einen von der Achsenkoordinate z unabhängigen Wert, da für $\lambda_0 = 0$ der vor dem Integral stehende Anteil sich zu R^2/A^2 errechnet. Bemerkenswerterweise erhält man als Integralwert des diffusiven Transports den Wert Null. Es gilt schliesslich:

$$Q = \pi R^2 w c_0.$$

Das ist gerade die durch den Zulauf zeitlich zugeführte Indikatormenge.

Aus der Gleichung (3) gewinnt man durch geeignete Konzentrationsmessung die Ausbreitungskennzahlen Bo_{tr} und Bo_l. Allerdings dürfte Bo_l einfacher durch eine Verdrängungsmessung zu bestimmen sein, so dass in diesem Fall nur noch Bo_{tr} aus der Gleichung (3) zu entnehmen ist.

Unter gewissen Bedingungen wird Gleichung (3) von Bo_l unabhängig. Entwickelt man nämlich den Exponenten und den Nenner der Reihenterme der Gleichung (3) in Potenzreihen,

$$\zeta Bo_l \left[\left(\tfrac{1}{4} + \frac{\lambda_\nu^2}{k^2 Bo_{tr} Bo_l}\right)^{1/2} - \tfrac{1}{2}\right] = \frac{\lambda_\nu^2 \zeta}{k^2 Bo_{tr}} \left(1 - \frac{\lambda_\nu^2}{k^2 Bo_{tr} Bo_l} \pm \dots\right),$$

$$\left(\tfrac{1}{4} + \frac{\lambda_\nu^2}{k^2 Bo_{tr} Bo_l}\right)^{1/2} + \tfrac{1}{2} = 1 + \frac{\lambda_\nu^2}{k^2 Bo_{tr} Bo_l} \mp \dots,$$

so wird klar, dass die Abhängigkeit von Bo_l für einen Einzelterm der Gleichung (3) entfällt, wenn in diesen Potenzreihen die zweiten Glieder klein gegen Eins sind. Dies (und überhaupt die Konvergenz der Potenzreihen) kann jedoch nur bis zu einem bestimmten λ_μ gelten. Soll nun die Unabhängigkeit von Bo_l für Gleichung (3) als Ganzes erfüllt sein, so müssen die Terme mit $\lambda_\nu > \lambda_\mu$ insgesamt schon klein sein gegen die vorigen, was im allgemeinen mit wachsendem $\zeta\lambda_\nu$ der Fall ist.

Kann man die genannten Bedingungen numerisch realisieren, so vereinfacht sich Gleichung (3) wie folgt:

$$y = 2\frac{R}{A} \sum_{\nu=0}^{\infty} \frac{J_1(\lambda_\nu R/A)}{\lambda_\nu J_0^2(\lambda_\nu)} \times \times J_0(\lambda_\nu \rho) \exp\left\{-\zeta \frac{\lambda_\nu^2}{k^2 Bo_{tr}}\right\}. \quad (4)$$

Bei unserem, in der Einleitung beschriebenen Messverfahren wird als mittlere Konzentration im Ausfluss gemessen:

$$\bar{y} = \frac{A^2}{\pi R^2} \int_{\phi=0}^{2\pi} \int_{\rho=0}^{R/A} y\rho\, d\rho\, d\phi = 4 \sum_{\nu=0}^{\infty} \frac{J_1^2(\lambda_\nu R/A)}{\lambda_\nu^2 J_0^2(\lambda_\nu)} \exp\left\{-\frac{L}{d} \frac{\lambda_\nu^2}{k^2 Bo_{tr}}\right\}. \quad (5)$$

Mit wachsendem Säulenradius nähert sich der Verlauf der Funktion dem Grenzwert für $R/A \to 0$. Der Grenzübergang ist nach folgender Umformung möglich:

$$\frac{R}{A}\lambda_\nu = \lambda_\nu^* \qquad \lambda_{\nu+1} - \lambda_\nu = \Delta\lambda_\nu$$

$$\frac{\Delta\lambda_\nu^*}{\Delta\lambda_\nu} = \frac{R}{A} \qquad \lambda_{\nu+1}^* - \lambda_\nu^* = \Delta\lambda_\nu^*$$

$$\bar{y} = 4 \sum_{\nu=0}^{\infty} \frac{J_1(\lambda_\nu^*)}{\lambda_\nu^*} \frac{\exp\{-\lambda_\nu^{*2}/(Bo_{tr} R^2/d\,.\,L)\}}{[\lambda_\nu^*/(R/A)]\, J_0^2[\lambda_\nu^*/(R/A)]} \frac{\Delta\lambda_\nu^*}{\Delta\lambda_\nu}.$$

Beim Grenzübergang $R/A \to 0$ sind nur solche von Null verschiedene $\lambda_\nu^* = \lambda_\nu R/A$ möglich, für die λ_ν gegen Unendlich strebt. Bei Grenzübergängen $\lambda \to \infty$ verhalten sich die Besselfunktionen wie

$$J_0(\lambda) = \sqrt{\left(\frac{2}{\pi\lambda}\right)} \cos(\lambda - \tfrac{1}{4}\pi),$$

$$J_1(\lambda) = \sqrt{\left(\frac{2}{\pi\lambda}\right)} \sin(\lambda - \tfrac{1}{4}\pi).$$

Mit $J_1(\lambda_\nu) = 0$ folgt $J_0(\lambda_\nu) = \sqrt{(2/\lambda_\nu \pi)}$ und $\Delta\lambda_\nu = \pi$.

VOL. 13 1961

Hiermit erhält man (nach der Definition des bestimmten Integrals)

$$\lim_{R/A \to 0} \bar{y} = 2 \int_0^\infty \frac{J_1^2(\lambda)}{\lambda} \exp\left\{ - \frac{\lambda^2}{\mathrm{Bo}_{tr}\, R^2/d\,.\,L} \right\} d\lambda.$$

Derselbe Grenzwert ergibt sich für $d/A \to 0$. Die Berechnung des uneigentlichen Integrals erfolgt über eine Potenzreihe:

$$J_1(\lambda) = \sum_{n=0}^{\infty} (-1)^n \frac{\lambda^{2n+1}}{2^{2n+1}\, n\,!\,(n+1)\,!},$$

$$J_1^2(\lambda) = \sum_{n=0}^{\infty} (-1)^n \frac{(2n+2)\,!\,\lambda^{2n+2}}{2^{2n+2}\, n\,!\,(n+2)\,!\,(n+1)\,!^2}$$

Folglich:

$$\bar{y} = 2 \sum_{n=0}^{\infty} (-1)^n \frac{(2n+2)\,!}{2^{2+2n}\, n\,!\,(n+2)\,!\,(n+1)\,!^2} \times \int_0^\infty \lambda^{2n+1} \exp\left\{ - \frac{\lambda^2}{\mathrm{Bo}_{tr}\, R^2/d\,.\,L} \right\} d\lambda,$$

oder wegen $\int_0^\infty \xi^{2n+1} \exp\left\{ - \frac{\xi^2}{a} \right\} d\xi = \frac{1}{2}\, n\,!\, a^{n+1}$:

$$\bar{y} = \tfrac{1}{4} \sum_{n=0}^{\infty} (-1)^n \frac{(2n+2)\,!}{2^{2n}(n+2)(n+1)\,!^2} \left(\frac{R^2}{d\,.\,L}\, \mathrm{Bo}_{tr} \right)^{n+1}$$

$$\bar{y} = \tfrac{1}{4} \sum_{n=0}^{\infty} (-1)^n\, a_n\, x^{n+1} \qquad (6)$$

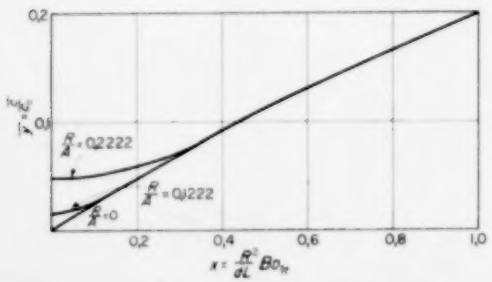

Abb. 2. Teildarstellung der Tabelle 1.

Tabelle 1. *Querausbreitung bei vernachlässigbarer Längsausbreitung*

x	$\bar{y} = \frac{\bar{c}}{c_0}$		
$= \frac{R^2}{d\,.\,L}\, \mathrm{Bo}_{tr}$	$\frac{R}{A} = 0{,}0000$	$\frac{R}{A} = 0{,}1222$	$\frac{R}{A} = 0{,}2222$
0,0000	0,0000	0,0149	0,0494
0,1000	0,0244	0,0247	0,0496
0,2000	0,0476	0,0476	0,0600
0,3000	0,0697		0,0720
0,4000	0,0908		0,0914
0,5000	0,1108		0,1111
0,6000	0,1300		0,1300
0,7000	0,1483		
0,8000	0,1661		
0,9000	0,1825		
1,0000	0,1986		
1,1000	0,2151		
1,2000	0,2285	wie bei $\frac{R}{A} = 0$	wie bei $\frac{R}{A} = 0$
1,3000	0,2426		
1,4000	0,2560		
1,5000	0,2690		
1,6000	0,2813		
1,7000	0,2933		
1,8000	0,3047		
1,9000	0,3157		
2,0000	0,3263		
2,5000	0,3741		
3,0000	0,4135		
4,0000	0,476		
5,0000	0,521		

mit

$$a_0 = 1,\ a_n = \frac{(2n+1)}{2\,(n+1)\,(n+2)}\, a_{n-1},\ x = \frac{R^2}{d\,.\,L}\, \mathrm{Bo}_{tr}.$$

Die Funktionsverläufe $\bar{y} = f(x, R/A)$ wurden aus Gleichung (6) für den Parameter $R/A = 0$ sowie aus Gleichung (5) für $R/A = 11/90$ und $R/A = 20/90$ berechnet und in Tabelle 1 und Diagramm Abb. 2 dargestellt. Mit Hilfe des Diagramms findet man die zu einer gemessenen mittleren Konzentration gehörende Ausbreitungskennzahl Bo_{tr}.

Formelzeichen

A = Säulenradius m

Bo_l = Longitudinale Bodensteinsche Kennzahl $= \dfrac{dw}{M_l}$

Bo_{tr} = Transversale Bodensteinsche Kennzahl $= \dfrac{dw}{M_{tr}}$

c = Örtlicher Wert der Indikatorkonzentration kg/m³

$\bar{c}$ = Über den Querschnitt der Säule gemittelte Konzentration kg/m³

c_0 = Indikatorkonzentration im Zulauf kg/m³

d = Für die Packung charakteristische Länge, z.B. Teilchengrösse m

$k = \dfrac{A}{d}$

L = Abstand zwischen Zulauf- und Entnahmeröhre m

λ_v = Entwicklungsparameter

M_l = Longitudinaler Mischungskoeffizient m²/sec

M_{tr} = Transversaler Mischungskoeffizient m²/sec

Q = Zeitlicher Durchfluss des Indikators durch den Säulenquerschnitt kg/sec

r = Radiale Zylinderkoordinate m

R = Radius der Zulauf- und Entnahmeröhre m

$\rho = \dfrac{r}{A}$

w = Mittlere Strömungsgeschwindigkeit in Achsenrichtung m/sec

$x = \dfrac{R^2}{L \cdot d}\,\mathrm{Bo}_{tr}$

$y = \dfrac{c}{c_0}$

$\bar{y} = \dfrac{\bar{c}}{c_0}$

z = Axiale Zylinderkoordinate m

$\zeta = \dfrac{z}{d}$

VOL. 13 1961

Literaturhinweise

[1] Klinkenberg A., Krajenbrink H. J. und Lauwerier H. A. *Industr. Engng. Chem.* 1953 **45** 1202.

[2] Hiby J. W. Quermischung in einphasig durchströmten Füllkörpersäulen, erscheint demnächst in *Chem. Ing. Tech.*

[3] Van Krevelen D. W. *Dechema-Monogr.* 1959 **32** 9.

Chemical Engineering Science, 1960, Vol. 13, pp. 75 to 81. Pergamon Press Ltd., London. Printed in Breat Gritain

Studies in optimization—III

The optimum operating conditions in sequences of stirred tank reactors

R. Aris

Department of Chemical Engineering, University of Minnesota, Minneapolis 14, Minnesota

(*Received* 8 *February* 1960)

Abstract—The problem of choosing the operating conditions, such as temperature and holding time, in a sequence of stirred tank reactors so as to maximize the profit from the conversion is here solved by a functional equation. This equation, derived by the method of dynamic programming, is very suitable for the repetitive calculations that a modern computing machine can perform. A general algorithm is given both in the case of a cascade of reactors and also when there is a by-passing of the original feed to later reactors.

Résumé—Présentation d'une équation fonctionnelle permettant de résoudre le problème du choix des conditions opératoires, telles que température et temps de rétension, dans une succession de réacteurs (avec mélange par agitation) pour obtenir un optimum de conversion. Cette équation, dérivée par la méthode de programmation dynamique est particulièrement convenable pour la répétition des calculs a effectuer avec un computeur moderne. Présentation d'un algorithme général convenant au cas d'une succession de réacteurs ainsi que lorsque l'alimentation primaire est partiellement court-circuitée aux réacteurs ultérieurs.

Zusammenfassung—Das Problem, die Reaktionsbedingungen, wie zum Beispiel die Temperatur und die Verweilzeit, in einer Rührkesselkaskade so zu wählen, dass der Reaktionsfortschritt auf einen Maximalwert ansteigt, wird hier durch eine funktionelle Gleichung gelöst. Diese Gleichung, die mit Hilfe der Methode der dynamischen Programmierung erhalten wurde, ist besonders für den wiederholenden Rechnungsgang geeignet, den die modernen Rechenmaschinen ausführen können. Ein allgemeines Zahlensystem wird angegeben, das sowohl für den Fall einer Rührkesselkaskade als auch für eine Rührkesselfolge gilt, bei der ein Teilstrom des ursprünglichen Frischzugangs den einzelnen Reaktoren zugeführt wird.

In an earlier paper [1] it was shown how the problem of choosing the optimum conditions in a sequence of stirred tank reactors could be solved by dynamic programming. The example discussed there was the very elegant one that Denbigh [2] devised to show the striking improvement of yield when two stages are held at different temperatures. It is the purpose of this paper to show how the same methods can be used to solve quite general optimum problems for the sequence of N stirred tank reactors. The presentation will be complete in itself, the earlier paper serving to give the picturesque detail of a particular example.

More recently Denbigh [3] has examined the optimum conditions in a sequence of reactors, in which the extent of reaction at any stage is controlled by the holding time or the amount of reactant added. He achieves the optimum by a method of " maximization of rectangles " drawn under a yield curve. It will readily be seen that this idea has considerable affinity with the notion of dynamic programming, in fact a simple and direct method of calculating his rectangles is to use a dynamic programme.

1. The Reaction System

We consider a system of m simultaneous reactions between the chemical species present. Since the reactions are independent it is always possible to choose a set of m chemical species which we will call the key components, and

associate each with one of the reactions. From the stoicheiometry of the reactions we may express the concentrations of all others in terms of these and of the reference composition from which the reaction mixture is derived. The rates of the reactions can be combined to give a function R_i, namely the rate of change of concentration of the i^{th} key component due to all the reactions. The R_i will be functions of the concentrations of all reactants and of the temperature, T. By the stoicheiometric relations they may be reduced to functions of $c_1, c_2 \ldots c_m$ and T and we write them $R_i(c_1, \ldots c_m, T) = R_i(c, T)$. The concentrations may be in mole or mass fractions, partial pressures or any other units suitable to the particular problem.

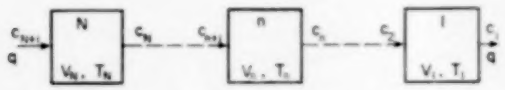

FIG. 1. The reactor system.

These reactions are to take place in a sequence of N reactors such as is shown in Fig. 1. It is convenient to number these from the last to the first so that the feed stream enters reactor N and the products leave reactor 1. We can quite consistently denote the concentrations within and leaving reactor n by c_{in} and the feed concentrations by $c_{i,N+1}$. The set of all concentrations c_{in}, $i = 1, 2, \ldots m$ will be denoted by c_n; this describes the state of the reactant stream leaving reactor n and entering reactor $(n-1)$. In any particular stage a choice of the operating variables, for example the holding time and temperature, must be made and these will affect the way in which the reactor transforms the state of the stream from c_{n+1} to c_n. If the flow rate of reactants is q a balance over the reactor gives

$$q(c_{in} - c_{i,n+1}) = V_n R_i(c_n, T_n) \qquad (1)$$
$$i = 1, 2, \ldots m$$

These m equations can be solved simultaneously to give c_n in terms of c_{n+1}. Let this be denoted by $c_n = \mathcal{T}_n(c_{n+1})$, where $\mathcal{T}_n$ is the transformation effected by reactor n and depends on the choice of the operating variables V_n and T_n. The composition of the product stream can be calculated from that of the feed repeated application of this,

$$c_1 = \mathcal{T}_1 \mathcal{T}_2 \mathcal{T}_3 \ldots \mathcal{T}_N(c_{N+1}) \qquad (2)$$

The overall transformation depends on the $2N$ variables V_n, T_n, $n = 1, 2, \ldots N$. In the case of a gas reaction the pressure might be taken as an operating variable, but the two chosen here will suffice.

A heat balance over reactor n gives the rate at which heat must be added or removed to maintain the operating temperature. Thus, if c_p and ρ are the specific heat and density of the reactants and H_i suitably defined heats of reaction,

$$qc_p\rho(T_n - T_{n+1}) = V_n \sum_1^m H_i R_i(c_n, T_n) - Q_n$$

where Q_n is the rate of heat removal. Then

$$Q_n = V_n \sum_1^m H_i R_i(c_n, T_n) - qc_p\rho(T_n - T_{n+1}) \qquad (3)$$

An optimum N-stage policy with respect to the state of the feed c_{N+1} is a choice of the $2N$ operating variables that maximizes a certain profit function. This profit function will represent the gain in value of the products over the raw material less the costs of operation. Let $v(c)$ be the value of a unit amount of the reaction mixture whose composition is c. Then the increase in value of the process stream per unit time is

$$q\{v(c_1) - v(c_{N+1})\}.$$

The operating cost, including the amortization of the initial cost, of any reactor is a function of its operating conditions, say $C(V_n, T_n)$. In the construction of this cost function we must take into account the best or current engineering practice, which will fix the cost of such items as the stirring of a vessel of volume V_n or the heat insulation of a reactor operating at T_n. There will also be a cost of pumping the reactant steam through the reactors and, assuming that it is not greatly affected by composition changes, this may be taken as a function of q, say $C'(q)$. The profit from an N stage reactor is thus

VOL. 13 1961

$$P_N(c_{N+1}, T_{N+1}; V, T; q) = q\{v(c_1) - v(c_{N+1})\} - \sum_1^N C(V_n, T_n) - C'(q) \quad (4)$$

and this may be calculated by equation (2) when $V_1, \ldots V_N$, $T_1, \ldots T_N$ and q are chosen. Thus when the operating conditions are fixed P_N becomes a function only of c_{N+1} and T_{N+1} and we may write

$$f_N(c_{N+1}, T_{N+1}) = \text{Max } P_N \quad (5)$$

The temperature of the feed T_{N+1} enters this expression since it is required to calculate the heat removed in reactor N and hence the cost of operating this stage. With certain simplified profit functions the feed temperature may not be important.

We observe that q enters this equation on rather a different basis from the other operating variables. This is because it is the same for all stages and it is convenient to think of it fixed. If we denote by Σp_n the profit per unit rate of flow without taking the pumping cost into consideration

$$P_N = q \sum_1^N p_n - C'(q)$$

where

$$p_n = v(c_n) - v(c_{n+1}) - \{C(V_n, T_n)/q\} \quad (6)$$

then we can determine first the maximum of Σp_n for any q and afterwards determine the q which will maximize P_N.

There will usually be certain physical restrictions on the choice of operating variables, such as the requirement that temperatures should not be too great. These can be expressed as inequalities and we will consider only T_n and V_n subject to

$$T_* \leqslant T_n \leqslant T^* \text{ and } V_* \leqslant V_n \leqslant V^* \quad (7)$$

2. The Principle of Optimality

The basic notion of dynamic programming has been enshrined by Bellman in the following words [4]: "An optimal policy has the property that whatever the initial state and initial decision are, the remaining decisions must constitute an optimal policy with regard to the state resulting from the first decision." In terms of our reactor system we may translate this to read: The optimal choice of operating conditions for N reactors with respect to the state c_{N+1}, T_{N+1} of the feed must be such that the conditions in reactors $(N-1)$, $(N-2), \ldots 2, 1$ constitute an optimum $(N-1)$ stage choice with respect to the state c_N, T_N. More coloquially, one must do the best one can with the output of the first reactor if there is to be any hope of achieving the best possible result from the complete set of N reactors. Moreover, if we know how to choose conditions optimally for an $(N-1)$ stage reactor we can find the optimal N stage policy by varying the conditions in the first reactor and always using the optimal $(N-1)$ stage policy with respect to the feed from the first reactor to the subsequent $(N-1)$ stages. The maximum over all such variations will give the best result for the N stage process and in this way we can build up the N stage policy a step at a time. At each step it is necessary to vary the operating conditions in only one stage. Since the amount of work required to find a maximum increases exponentially with the number of simultaneously varied quantities the principle of optimality has saved a tremendous amount of work and introduced a vital organization into the calculation.

For any particular q let

$$g_N(c_{N+1}, T_{N+1}) = \text{Max} \left(\sum_1^N p_n\right) \quad (8)$$

where the maximization is by correct choice of V_n, T_n, $n = 1, 2, \ldots N$. Then a mathematical transliteration of the principle of optimality gives

$$g_N(c_{N+1}, T_{N+1}) = \text{Max}\{p_N + g_{N-1}(c_N, T_N)\} \quad (9)$$

where this time maximization requires only the correct choice of V_N and T_N. At any stage we can find f_N, for

$$f_N(c_{N+1}, T_{N+1}) = \text{Max}\{q\, g_N(c_{N+1}, T_{N+1}) - C'(q)\} \quad (10)$$

the maximization being for a correct choice of q.

Although in analysing an N stage process with respect to a particular feed state we are forced to consider policies with respect to other feeds

this extra information is of interest and importance. It would be a short-sighted analysis that did not consider the effect of variations in the feed state on the optimum policy, and though there is an optimal value of q it is not always possible to use it.

3. The Calculation and Presentation of Results

The principle of optimality has given us a functional equation to solve. Set out in full the system of equations is

$$g_N(c_{N+1}, T_{N+1}) = \text{Max}\{p_N + g_{N-1}(c_N, T_N)\} \quad (11)$$

where

$$p_N = v(c_N) - v(c_{N+1}) - C(V_N, T_N) \quad (12)$$

and

$$c_N = \mathcal{F}_N(c_{N+1}) \quad (13)$$

$\mathcal{F}_N$ is the solution of the equations (1) and in calculating the cost function $C(V_N, T_N)$ equation (3) is needed to give the cost of heating or cooling the reactor. The sequence of equations is started by observing that

$$g_0 = 0$$

and so

$$g_1(c_2, T_2) = \text{Max}\{p_1\} \quad (14)$$

The modern digital computer is well suited to repetitive calculations of this type, for it can be programmed to do the calculation for given N, print out the results, store g_N in the place where g_{N-1} was before and then go through to same cycle of calculation to get g_{N+1}. The machine looks for the maximum by direct calculation, and inequality restrictions, such as (7), actually help by confining the area of search. The chief difficulty lies in storing a function of $(m + 1)$ variables and this may be prohibitive if m is not small. Two devices, both of which are used in the earlier paper [1] can be used to cut down the work and storage required. Firstly if all the reactions are first order the equations (1) will be homogeneous in the c_i. It is then possible to work with the ratio of the concentrations to any one of them, say c_m, and this reduces the number of variables by one. Secondly, it may be that the temperature enters the rate expressions R_i only in the form of a rate constant $k_i \exp(-E_i/RT)$. In this case if we are not concerned with costs dependent on temperature it is convenient to take one of these rate constants as an independent variable. All the other constants can be expressed as powers of this one and the maximizations with respect to T may be performed by varying this rate constant. This is perfectly satisfactory since $\exp(-E/RT)$ is a monotonic function of T.

The results of each step of the calculation may be tabulated as shown below:

These tables are prepared one after the other by solving the equations (11), (12) and (13). Given any feed c_{N+1}, T_{N+1} we can find the complete optimum policy as follows. First by entering the table for $n = N$ at c_{N+1}, T_{N+1} we have the optimum profit function $g_N(c_{N+1}, T_{N+1})$ and the operating conditions, V_N, T_N, for the first stage. The final columns give the state of the stream produced under these optimum conditions. Since the principle of optimality states that the remaining $(N - 1)$ stages must use optimal policy we can find the operating conditions in the second reactor by entering the table for $n = N - 1$ at c_N, T_N. This will give V_{N-1}, T_{N-1} and the resulting state c_{N-1}, T_{N-1} which is the feed to the remaining $(N - 2)$ stages. Passing through the

Number of reactor from end: n

Feed state	Optimum profit function	Optimal operating conditions	Exit state under these conditions
c_{n+1}, T_{n+1}	$g_n(c_{n+1}, T_{n+1})$	V_n, T_n	c_n, T_n

VOL. 13 1961

tables in this way the complete optimum design may be rapidly extracted.

4. The Notion of the Lagrange Multiplier

In the general profit function described above a definite cost was associated with the volume of the reactor. It might happen however that the interesting problem is to determine the maximum yield of a particular component with little or no regard to the costs of operation. In some cases a physical restriction will still have to be imposed. For example with a reversible reaction the greatest yield will be the equilibrium yield at the most favourable temperature but it will require an infinite volume of reactor to achieve this. We are thus interested in the optimum yield for a fixed total reactor volume V. This can be expressed by explicitly letting the optimum yield be a function of V; thus if c is the concentration of the product we let

$$f_N(c_{N+1}, V) = \text{Max}\{c_1 - c_{N+1}\} \qquad (15)$$

the maximization being over choice of $T_1, T_2, \ldots T_N$ and $V_1, V_2, \ldots V_N$ subject to

$$V_1 + V_2 + V_3 + \ldots V_N = V \qquad (16)$$

The principle of optimality then gives

$$f_N(c_{N+1}, V) = \text{Max}\{c_N - c_{N+1} + f_{N-1}(c_N, V - V_N)\} \qquad (17)$$

the maximization being over choice of T_N and V_N subject to $V_N \leqslant V$. Here, however, the function f_N is a function of two arguments and the storage and interpolation of such a function is much more troublesome than that of a single variable.

Another approach to this problem is to construct an artificial cost function associated with the volume and to maximize this slightly more general profit function. Thus in this case we would consider the profit function

$$P_N = q(c_1 - c_{N+1}) - \mu \sum_1^N V_n = q \sum_1^N p_n \qquad (18)$$

where

$$p_n = c_n - c_{n+1} - \mu t_n, \quad t_n = V_n/q$$

and μ is any positive constant. Now if

$$g_N(c_{N+1}) = \text{Max} \sum_1^N p_n \qquad (19)$$

we have no need to make g_N a function of ΣV_n for the maximum will occur at a finite total volume. In fact now $V = \sum_1^N V_n$ is a function of μ, for the equation for g_N, namely

$$g_N(c_{N+1}) = \text{Max}\{p_N + g_{N-1}(c_N)\} \qquad (20)$$

can be solved for any N, μ and c_{N+1} and the total volume calculated. For a given feed state V is such a function of μ and N as is shown in Fig. 2. It is now possible to choose the value of μ so that the total volume will be as required. μ is called the Lagrange multiplier and is in fact a cost associated with the volume so that the larger μ is the smaller will be the optimum volume. This way of putting the problem is often of great advantage in saving computer storage and time.

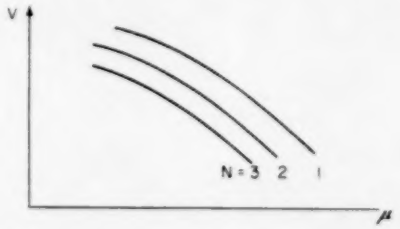

Fig. 2. Dependence of the total volume on the Lagrange multiplier μ.

The Lagrange multiplier can also be adapted to other situations. If, for example, we seek the policy for an N stage process which gives the greatest space–time yield $(c_1 - c_{N+1})/\sum_1^N V_n$ it is computationally easier to solve the problem defined by (18), (19) and (20) and afterwards find the value of μ which maximizes the space–time yield. The same technique can be employed if we seek to maximize the fraction of one of the reactants which is converted into a particular product. The value function $v(c)$ can also be used to include specification requirements on the product. Thus if the concentration of a particular component is required to lie in a certain interval $v(c)$ can be put equal to zero outside this interval.

5. Optimum Policy with By-passing of Feed

As an extension of the general programme it is interesting to see how to find the optimum policy with by-passing of feed to later stages of the process. The system is as shown in Fig. 3, at stage n we have not only the product of the previous

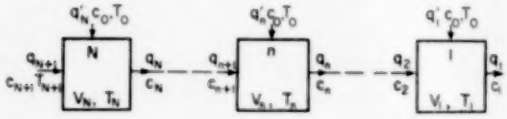

FIG. 3. The reactor system with by-passing.

stage $(n+1)$ coming in with flow rate q_{n+1}, but also added, fresh feed of fixed composition c_0 at a rate q_n'. The mass and heat balances now read

$$q_n = q_n' + q_{n+1} \tag{21}$$

$$q_n c_{in} - q_{n+1} c_{i,n+1} - q_n' c_{i0} = V_n R_i(c_n, T_n) \tag{22}$$

$$q_n T_n - q_{n+1} T_{n+1} - q_n' T_0 = V_n \sum_1^m h_i R_i(c_n, T_n) - q_1 Q_n^* \tag{23}$$

where $h_i = H_i/c_p \rho$ and $q_1 Q_n^* = Q_n/c_p \rho$. The operating conditions at each stage are now not only V_n and T_n but also q_n'.

We may again write a general profit function in the same form as (4) above:

$$P_N(c_{N+1}, T_{N+1};\ c_0, T_0;\ V, T, q';\ q_1) = q_1 v(c_1) - q_{N+1} v(c_{N+1}) - \left(\sum_1^N q_n'\right) v(c_0) - \sum_1^N C(V_n, T_n) - C'(q_1) \tag{24}$$

where $C'(q_1)$ is the estimate of the cost of pumping in terms of the final flow rate. As before q_1 enters in rather a different fashion from the other variables since all else depends only on the ratio of the flow rates. We shall again adopt the technique of seeking first the maximum of $\{P_N + C'(q_1)\}/q_1 = \sum_1^N p_n$ and afterwards choosing q_1 to maximize P_N. At the expense of a little more complication however it would not be difficult to include the individual pumping costs of all side streams.

Let $\lambda_n = q_n/q_1$, $\lambda_n' = q_n'/q_1 = \lambda_n - \lambda_{n+1}$ and

$$\begin{aligned} p_n &= \lambda_n v(c_n) - \lambda_{n+1} v(c_{n+1}) - \\ &\quad - \lambda_n' v(c_0) - \{C(V_n, T_n)/q_1\} \\ &= \lambda_n \{v(c_n) - v(c_0)\} - \lambda_{n+1} \\ &\quad \{v(c_{n+1}) - v(c_0)\} - \{C(V_n, T_n)/q_1\} \end{aligned} \tag{25}$$

Then if

$$g_N(c_{N+1}, T_{N+1};\ c_0, T_0) = \operatorname{Max} \sum_1^N p_n \tag{26}$$

the maximization is over suitable choice of $V_1, \ldots V_N$, $T_1, \ldots T_N$ and $\lambda_2, \ldots \lambda_{N+1}$ subject to $\lambda_{N+1} \leqslant \lambda_N \leqslant \ldots \leqslant \lambda_2 \leqslant \lambda_1 = 1$. We should not at this stage identify the feed composition c_{N+1} with c_0 for we have to set up a functional equation for g_N as a function of its first two arguments. At the final stage we can identify c_{N+1} and c_0 and then of course λ_{N+1} loses its meaning. The presentation also allows for the by-pass feeds being of different composition from the original feed: it would be possible to have arbitrary compositions for all these feeds but it would involve carrying along many more variables. When the meaning is quite clear we can write g_N as a function of its first two arguments only.

If we write $t_n = V_n/q_1$ as the "holding time" of stage n, then equations (22) and (23) are

$$\lambda_n(c_{in} - c_{i0}) - \lambda_{n+1}(c_{i,n+1}' - c_{i0}) = t_n R_i(c_n, T_n) \tag{27}$$

$$\lambda_n(T_n - T_0) - \lambda_{n+1}(T_{n+1} - T_0) = t_n \sum_1^m h_i R_i(c_n, T_n) - Q_n^* \tag{28}$$

Applying the principle of optimality to g_N we have

$$g_N(c_{N+1}, T_{N+1}) = \operatorname{Max}\{p_N + g_{N-1}(c_N, T_N)\} \tag{29}$$

where the maximization is over suitable choice of T_N, t_N and λ_{N+1}. T_N and t_N may be restricted by such inequalities as (7) and λ_{N+1} is less than or equal to λ_N which is known from the calculation of g_{N-1}. The sequence of equations is started with

$$g_1(c_2, T_2) = \operatorname{Max}\{p_1\}, \quad \lambda_1 = 1.$$

The case where the only heat supplied is in initially heating the feed to reactor N, and a

VOL. 13 1961

falling temperature sequence is obtained by by-passing cold feed, is of particular simplicity and interest; it will be considered in detail in a later paper [5]. Sufficient has been said here to show the suitability of dynamic programming for the whole range of optimum problems with sequences of stirred tanks.

Acknowledgement—I am indebted to Professor K. G. Denbigh for his interest in this topic and for showing me his contribution to the Amsterdam conference whilst it was still in manuscript.

Notation

$C(V_n, T_n)$ = cost of operating reactor n as a function of its volume and temperature
$C'(q)$ = cost of pumping at rate q
c_i = concentration of i^{th} key species
c_p = specific heat of reaction mixture
$f_N(c_{N+1}, T_{N+1})$ = maximum profit from N reactors with feed state c_{N+1}, T_{N+1}
$i_N(c_{N+1}, T_{N+1})$ = Max Σp_n
H_i = heat of i^{th} reaction
N = number of reactors
$P_N = q\{v(c_1) - v(c_{N+1})\} - \sum_1^N C(V_n, T_n) - C'(q)$
$p_n = v(c_n) - v(c_{n+1}) - \{C(V_n, T_n)/q\}$
Q_n = rate of heat removal from n^{th} reactor
q = flow rate through all reactors (sections 1–4)
q_n = flow from reactor n
q_n' = by-pass flow rate to n^{th} reactor
R_i = rate of change of c_i due to all reactions
T_n = temperature of reactor n
$t_n = V_n/q$, holding time of reactor n
V_n = volume of reactor n
$v(c)$ = value of unit volume of reaction mixture of composition c
$\lambda_n = q_n/q_1$
$\lambda'_n = q_n'/q_1 = \lambda_n - \lambda_{n+1}$
ρ = density of reaction mixture

References

[1] Aris R. *Chem. Engng. Sci.* 1960 **12** 56.

[2] Denbigh K. G. *Chem. Engng. Sci.* 1958 **8** 125.

[3] Denbigh K. G. Contribution to the 2*nd Amsterdam Conference on Reactor Design Engineering* 1960, to be published.

[4] Bellman R. *Dynamic Programming*. Princeton University Press, Princeton 1957.

[5] Aris R. Contribution to the *Symposium on Optimization in Chemical Engineering*. New York University, New York, May 1960.

Chemical Engineering Science, 1960, Vol. 13, pp. 82 to 89. Pergamon Press Ltd., London. Printed in Great Britain

The separation of volatile liquid mixtures by continuous gas–liquid chromatography

P. E. Barker and D. Critcher

Department of Chemical Engineering, University of Birmingham

(*Received* 27 *February* 1960; *in revised form* 12 *May* 1960)

Abstract—A process is described for the separation of binary liquid mixtures by a method which is fundamentally the same as extractive distillation but uses a finely divided solid as a carrier for the non-volatile solvent. A non-volatile solvent absorbed on the surface of crushed kieselguhr flows down a column countercurrent to a stream of air. The mixture to be separated is injected continuously as a liquid feed into the mid-point of the column. The flows of gas and solid are adjusted such that one component is carried upwards in the gas stream and the other component downwards absorbed in the non-volatile liquid. Benzene and *cyclo*hexane have been successfully separated at a rate of 30 cm³/hr in a 1 in. diameter column 4 ft long when using polyoxyethylene 400 di-ricinoleate as the non-volatile solvent. The H.T.U. (height of transfer unit) for this system and column packing was found to be approximately 2 cm.

Résumé—Les auteurs décrivent un procédé de séparation de mélanges liquides binaires par une méthode semblable à celle de la distillation extractive mais utilisant un solide finement divisé comme support du solvant non volatil. Un solvant non volatil absorbé par du kieselguhr concassé s'écoule du haut vers le bas d'une colonne, à contre-courant d'un écoulement d'air. Le mélange à séparer est injecté de façon continue dans le milieu de la colonne. Les débits du gaz et du solide sont établis de telle sorte qu'un composant est entraîné vers le haut par le courant gazeux tandis que, l'autre absorbé par le liquide non volatil, s'écoule vers le bas. Une bonne séparation de benzène et de cyclohexane a été faite, à une vitesse de 30 cm³/h dans une colonne de 1 pouce de diamètre et 4 pieds de haut en utilisant comme solvant non volatil du polyoxyethylène 400 di-ricinoleate. La hauteur d'unité de transfert (HTU) pour ce système et le garnissage de cette colonne est de 2 cm environ.

Zusammenfassung—Es wird ein Prozess zur Trennung binärer Flüssigkeitsgemische beschrieben. Diese Trennung wird durch eine Methode erreicht, die grundsätzlich dasselbe wie eine extraktive Destillation darstellt, bei der aber ein fein verteilter Feststoff als Träger für ein nichtflüchtiges Lösungsmittel dient. Dieses nichtflüchtige Lösungsmittel, das auf der Oberfläche von gemahlener Kieselgur adsorbiert ist, fliesst in einer Säule entgegen einem Luftstrom nach unten. Das zu trennende Gemisch wird kontinuierlich als Flüssigkeit im Mittelpunkt der Säule eingeführt. Der Gas- und Flüssigkeitsstrom wird so eingestellt, dass eine Komponente im Gasstrom nach oben und die andere in der nichtflüchtigen Flüssigkeit absorbiert nach unten geführt wird. Benzol und Cyclohexan wurden erfolgreich getrennt bei einer Zuflussgeschwindigkeit von 30 cm³/h in einer 120 cm langen Säule von 2,5 cm Durchmesser. Dabei wurde Polyoxyaethylen (400)-di-ricinoleat als nichtflüchtiges Lösungsmittel verwendet. Es wurde gefunden, dass die HTU (Höhe einer Übertragungseinheit) für dieses System bei der angegebenen Säulenfüllung etwa 2 cm beträgt.

1. Introduction

Much interest has been aroused in recent years in the use of gas–liquid chromatography (G–L–C) as a means of analysing mixtures of volatile liquids and gases. In this technique the mixture to be analysed is vaporized into a stream of inert gas which passes through a column containing a non-volatile liquid absorbed on the surface of a finely divided solid. Due to the differences in volatility of the solute and/or physical interaction in the non-volatile liquid phase, separation into pure constituents occurs as bands within the column. The different constituents are eluted from the column by the moving gas stream. A detector placed at the outlet from the column indicates the time of elution and also the concentration of the component thus enabling qualitative and quantitative analyses to be made.

The use of large scale G–L–C columns up to 3 in. diameter to increase the quantity to be separated at any one time has been fully investigated [1, 2, 3, 4]. A semi-continuous unit has been produced commercially in which the next batch of material is injected into the column as

VOL. 13 1961

the last component from the previous batch is eluted [5].

The purpose of this work has been to study a countercurrent analogue of G–L–C. That is to allow a solid containing an absorbed solvent to move countercurrently to an inert gas stream and to inject a liquid feed continuously into the mid-point of the column. By using this technique it was hoped to achieve difficult separations of volatile liquids and gases on a much greater scale than has been possible with G–L–C columns.

This countercurrent analogue of G–L–C can be considered to be extractive distillation [6] since the solid acts merely as a carrier and takes no part in the diffusional processes occuring. A continuous process operating in the above manner and using a vapour feed has been used to separate aromatic hydrocarbons from coal gas [7]. The countercurrent analogue of gas adsorption chromatography, hypersorption, [8, 9] has been practised on a commercial scale for just over a decade.

2. Theory

This method, like other processes for separating different compounds is dependent upon the components distributing themselves differently between two phases. In this case the phases are air and a non-volatile solvent absorbed on the surface of suitable solid such as kieselguhr. The solid acts as a carrier and takes no part in the separation.

Each phase has a preferential selectivity for one or other of the solute components. Movement of two phases countercurrently will produce in each phase a relatively high concentration of one solute and a relatively low concentration of the other, so that given a sufficient height of column a substantially complete separation is possible.

The suitability of a solvent for a given separation together with conditions of operation may be seen from a chromatogram of the binary mixture (AB) obtained on a gas-liquid chromatography apparatus (Fig. 1).

The linear velocity of component A through the column is z/R_A where z is the length of the column and R_A the retention time of component A. Similarly the velocity of B is z/R_B. Thus if the column packing is moved countercurrently to the carrier gas stream at a velocity greater than z/R_A but less than z/R_B component B will be carried in the direction of the packing absorbed in the liquid phase. Component A will be eluted in the carrier gas.

It is more convenient to express the conditions of separation in terms of the volume flow of solvent and carrier gas rather than linear velocities.

The partition coefficient, k, for a particular component may be defined as

$$\frac{\text{Weight of component per unit volume of solvent phase}}{\text{Weight of component per unit volume of carrier gas phase}}$$

Let the partition coefficients of components A and B at the temperature of the rectification section of the column be k_A^R and k_B^R respectively

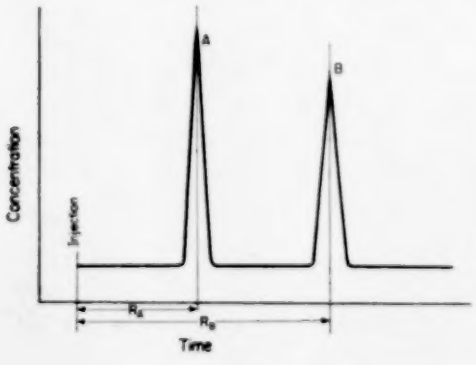

Fig. 1.

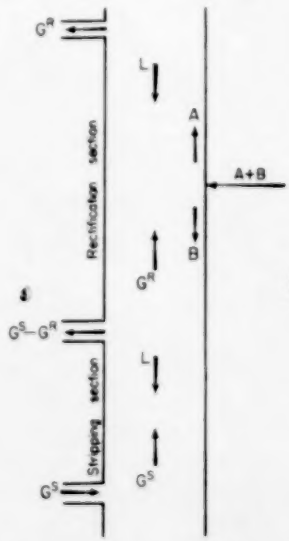

Fig. 2.

(see Fig. 2). If component B has the longer retention time in the stationary column, then k_B^R will be greater than k_A^R.

Let the volume flow rates of solvent and carrier gas in the rectification section be L and G^R respectively. These may be considered constant when the temperature of the column is kept constant, and the pressure drop across the column is small.

For component A to move in the direction of the gas phase G^R/L must be greater than k_A^R. Similarly for component B to move in the direction of the liquid phase, G^R/L must be less than k_B^R.

The condition for separation is

$$k_A^R < \frac{G^R}{L} < k_B^R$$

Thus there will be a range of possible operating values of G_R/L over which separation may be obtained. In the ideal case complete separation would be achieved over the whole range of values of G_R/L from k_A^R to k_B^R. The actual operating values may only approach the respective k values, the degree of approach being dependent upon the column size and its efficiency.

For component B to be stripped from the liquid phase, the ratio of carrier gas flow to solvent flow in the stripping section for the ideal case is given by

$$\frac{G^S}{L} > k_B^S$$

where k_B^S is the partition coefficient of component B at the temperature of operation of the stripping section, and G^S is the carrier gas flow rate in that section. The operating value of G^S/L must be much greater than k_B^S in order to recover all of component B from the liquid phase. The actual value will again depend on the column size and its efficiency.

3. Experimental

Materials used

One of the advantages of this process over simple distillation is that separations can be achieved by differences in polarity as well as boiling point. Polar molecules are those in which the charge density is not uniform over the surface of the molecule but is concentrated at one or two points. The method can therefore appropriately be demonstrated by separating two liquids with approximately the same boiling point, but of different polarity. With this in mind preliminary work has been carried out using a polyglycol derivative (polyoxyethylene 400 di-ricinoleate) absorbed on 10/20 mesh kieselguhr to separate benzene (b.p. 80·1°C) and *cyclo*hexane (b.p. 80·7°C).

Equilibrium data determinations

To permit the estimation of the relative flow rates of packing and carrier gas the partition coefficients of benzene and *cyclo*hexane between the solvent and air at various temperatures were determined. Measurements of retention times were made on a standard G–L–C unit, using a 4 mm diameter column, 5 ft in length, packed with 40–60 mesh C22 fire-brick containing 25 per cent by weight of polyoxyethylene 400 di-ricinoleate. Air was used as the carrier gas, with a katharometer as the detecting element. The partition coefficients were calculated from the following equation derived by James and Martin [10].

$$k = \frac{A_L}{A_S}\left\{\frac{3V_R}{2A_L z}\left[\frac{(P_i/P_0)^2 - 1}{(P_i/P_0)^3 - 1}\right] - 1\right\}$$

where A_L = cross-sectional area occupied by the mobile phase
A_S = cross-sectional area occupied by the stationary phase
V_R = retention volume to the centre of the zone
z = length of column
P_i = pressure at column inlet
P_0 = pressure at column outlet

Values of the partition coefficients at various temperatures are shown in Table 1. It was found that the partition coefficients could be expressed by the following equations:

$$\text{For benzene } \log_{10} k = \frac{1440}{\theta} - 1{\cdot}975$$

$$\text{For } \textit{cyclo}\text{hexane } \log_{10} k = \frac{1230}{\theta} - 1{\cdot}719$$

where k = the partition coefficient, θ = °Kelvin.

Table 1

Temperature (°C)	*K values for benzene*	*K values for cyclohexane*	*Ratio* $\frac{\text{benzene}}{\text{cyclohexane}}$
20	885	298	2·99
40	430	159	2·70
60	210	87	2·42
80	128	57	2·24
100	75	37	2·03

General description of apparatus

The flow diagram of the apparatus is shown in Fig. 3. A sealed reservior (A) containing the packing was placed at the top of the 1 in. diameter column, the flow being controlled by means of a feed table (B) at the bottom of the column. Air was supplied to the column below the stripping section (C) and was drawn through under vacuum. The air was dried, preheated in (D) to aid the stripping and supplied at a pressure slightly above atmospheric. This ensured a flow of air out from the bottom of the column so preventing any moisture entering the system.

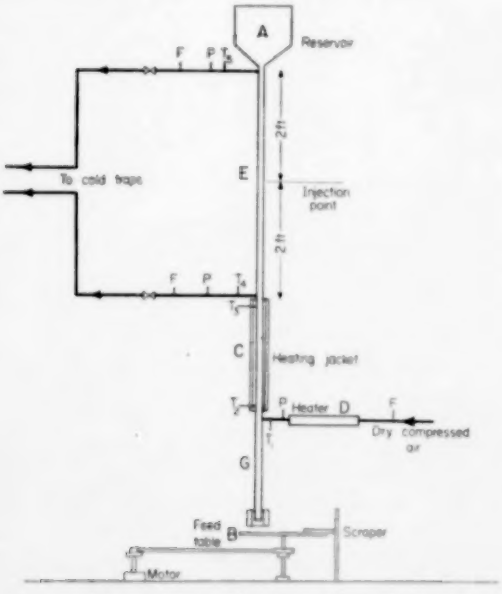

Fig. 3. Flow diagram of apparatus
T **Temperature measurement**
P **Pressure temperature**
F **Flow measurement**

The mixture to be separated was injected at the mid-point of the rectification section (E). The more strongly absorbed component was carried down in the liquid phase and was removed from the column by an excess of air in the stripping section (C). The less strongly absorbed component was carried upwards in the gas phase. Both streams passed through cold traps to condense out the separated products.

Column construction

The glass column was divided into four sections, the rectification section (E) being 4 ft in length and the stripping section (C) 2 ft. The section below the stripper (G) which allowed the packing to cool before leaving the column was 18 in. in length. The stripping section was enclosed in an air jacket contained by the column and a concentric glass tube, 2 in. in diameter, on which several turns of resistance wire were wound. A further concentric tube, 3 in. in diameter, served to eliminate the effect of draughts.

Flow of packing

The support used was Johns–Manville C22 firebrick ground approximately to 10–20 B.S. mesh and carrying 24·9 per cent w/w of liquid phase. The sieve analysis at the commencement of the runs is shown in Table 2.

The packing flowed under gravity from a sealed reservoir which contained a supply lasting 4–6 hr, depending on the flow rate. The rate of discharge was independent of the head unless the reservoir was nearly empty. To avoid irregular flow of the packing it was necessary to vibrate the column. This was achieved by means of an electric bell impinging on the column just below the stripping section.

The packing discharged through an orifice at the bottom of the column on to a rotating table, which was driven through a gear system by a variable speed motor. A range of speeds from 1–4 rev/min was possible. The packing was removed from the table by a scraper. The position of the table relative to the column outlet could be varied, so increasing or decreasing the rate of removal of the packing.

Details of the orifice at the bottom of the

column are shown in Fig. 4. The flow rates were found to be too high when the width of the solid band removed was greater than 0·5 in. and the conical section was introduced to reduce the diameter of the column. The height of the orifice above the table could be varied to control the depth of packing removed and orifices ranging from 0·25–0·5 in. were used to vary the width of the solid band.

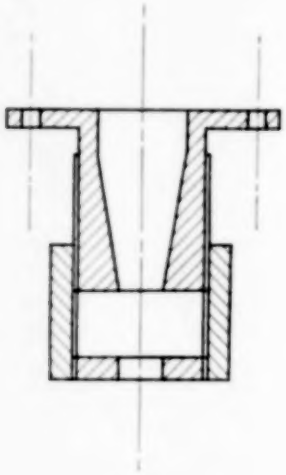

Fig. 4.

Thus the flow rate could be controlled or varied in the following ways:

(a) Speed of the feed table.
(b) Position of the feed table relative to the column outlet.
(c) Height of the orifice above the feed table.
(d) Size of the orifice.

Air supply flow, temperature and pressure measurement

Silica gel was used to remove any moisture in the entering air which was preheated to aid the stripping process.

The flow of air to the column was indicated by a rotameter between the drier and heater. The temperature and pressure were measured at the column inlet. The flows of air from the column were measured by capillary flowmeters. The temperature and pressure of both streams were measured at the column outlets.

Injection and collection

The mixture to be separated was injected by means of a micro-pump through a hole, $\frac{1}{64}$ in. in diameter, in a brass flange which was inserted between the two sections of the rectification column. A small heater around the inlet feed pipe ensured vaporization of the liquid into the air stream. The maximum capacity of the micro-pump was 40 cm^3/hr.

The products were recovered in cold traps which could be by-passed during the initial stages of a run, each outlet stream from the column passing through two such traps. The first trap contained solid carbon dioxide, the second solid carbon dioxide in acetone. The first trap at a temperature of -20°C condensed out most of the liquid but a second trap at -80°C was was necessary to recover 95 per cent of the material fed into the column, the remainder passing through the traps to the vacuum pump.

Table 2

Sieve analysis of starting material		*Sieve analysis of brick after being recycled approximately eight times*	
B.S. mesh	% *Wt.*	*B.S. mesh*	% *Wt*
8	0·24	8	0·14
8–10	32·60	8–10	18·51
10–12	13·23	10–12	9·56
12–14	22·47	12–14	19·96
14–16	21·60	14–16	32·28
16–18	9·26	16–18	17·27
18–25	0·41	18–25	0·79
25	0·19	25	1·50

Experimental procedure

The air jacket surrounding the stripping column was allowed to attain the required temperature, with air flowing through the column. The feed table was then started and the gas flows adjusted to the required values. The pressure at the inlet to the stripper was maintained at approxinately 5 cm water-gauge. Once the flows were steady injection was commenced. The apparatus was run for about 30 min to reach steady conditions after which the outlet streams from the column

VOL 13 196

were diverted through the cold traps. Since sample volumes of 10 cm³ were sufficient for analytical purposes the length of each run depended on the injection rate. The solid support was collected throughout this period and the average flow rate determined.

Analysis

The samples were analysed by gas–liquid chromatography, using the column described previously, but with nitrogen as the carrier gas. By increasing the sample size concentrations down to 0·1 per cent could be detected.

4. Results and Discussion

Complete separation of benzene and *cyclo*hexane has been achieved over a wide range of operating conditions, the results being summarized in Fig. 5. The lines *AB* and *CD* show the limiting values of air and solid flows for complete separation. Complete data for three of the runs are shown in Table 3. The injection rate was maintained at 30 cm³/hr throughout this series of experiments; the air flow and temperatures through the stripping section also remained constant.

At an injection rate of 30 cm³/hr and an air flow rate of 50 l/hr the air was saturated with vapour around the feed point, and the packing appeared moist for some distance below the injection point, though separation was accomplished at lower air rates. The flow rates of air and solid obtainable with the present design limit the throughput to 40 cm³/hr. At higher air and solid rates, complete separation occurred over a range of G/L values from 300 to 750. As saturation was approached this range was reduced to 350 to 700. The limiting values of G/L for separation were predicted as 300 and 900 at 20°C as can be seen from Table 1. Benzene appeared in the top product when G/L was approximately 700, showing that the number of theoretical stages above the injection point was insufficient to remove all the benzene from the gas phase. Below the injection point the rectification section followed the predicted value of G/L, i.e.

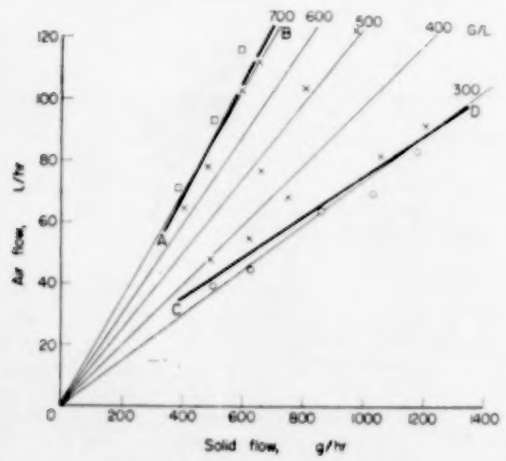

Fig. 5. × complete separation
O *cyclo*hexane in bottom product
□ benzene in top product.

Table 3

Run number	1	2	3
Air flow in rectification section (l/hr)	44·2	76·9	115·7
Air flow from stripping section (l/hr)	109·9	106·3	101·3
Air flow to column (l/hr)	232	257	257
Outlet pressure : rectification section (mm Hg)	744	739·5	728
Outlet pressure : stripping section	746·8	746·3	744·5
Inlet pressure : stripping section (mm Hg)	764·9	764·8	764·2
Solid flow (g/hr)	630	665	600
Injection rate (cm³/hr)	30	30	30
Temperatures T_1 (°C)	91	89	94
T_2 (°C)	99	94	97
T_3 (°C)	92	84	89
T_4 (°C)	55	54	65
T_5 (°C)	20	19·5	20
Overhead product : *cyclo*hexane (% vol.)	99·9	99·9	98·9
Bottom product : benzene (% vol.)	99·2	99·9	99·9

*cyclo*hexane appeared in the bottom product when G/L was approximately 300. The apparent higher efficiency in this section was due to the fact that the air entered the rectification section at a temperature of about 60°C. The partition coefficient for *cyclo*hexane at this temperature was 87, and the condition for *cyclo*hexane to move in the direction of the gas phase was that the G/L be greater than 87. The operating range over which separation was achieved was thus increased by the temperature gradient existing at the bottom of the rectification section.

It is apparent that a rectification section of 4 ft in length is capable of separating a system having a partition coefficient ratio less than that of benzene/*cyclo*hexane.

Evaluation of column efficiency

By definition for dilute systems "the number of over-all gas phase transfer units," N_{OG}, with reference to the heavy component benzene, is given by equation (1)

$$N_{OG} = \int_{y_2}^{y_1} \frac{dy}{y - y_e} \qquad (1)$$

For a particular absorption column of packed height Z the number of transfer units and the height of a transfer unit are related

$$Z = H_{OG} \times N_{OG} \qquad (2)$$

If the equilibrium line is linear N_{OG} can be calculated from the terminal concentrations

$$N_{OG} = \frac{(y_1 - y_2)}{(y - y_e)_{L.M.}} \qquad (3)$$

For the experimental conditions of this investigation the resistance to mass transfer resides in the gas phase due to the high solubility of the solutes in the solvent; any resistance in the liquid phase may be neglected.

Under these conditions

$$H_{OG} = H_G$$
$$N_{OG} = N_G$$

To illustrate the method a set of conditions has been chosen from the line AB on Fig. 5 which represents the upper limit of air flow for a given solid flow, i.e. benzene was beginning to appear in the top product and the column above the feed could be assumed to be working completely. A temperature of 20°C and an injection rate of 30 cm³/hr have been assumed similar to the experiments recorded in Fig. 5. Shown plotted on Fig. 6 are the equilibrium line for benzene at 20°C and the operating line for benzene in the section of the column above the feed point, at column conditions indicated in Table 4. The purity of the *cyclo*hexane at the top of the column has been taken as 99·9 per cent.

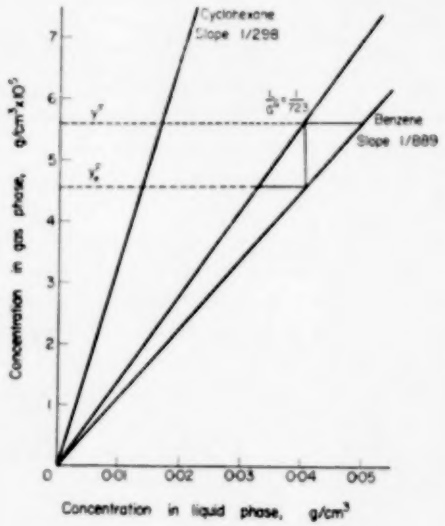

Fig. 6.

Table 4

Air flow rate	(l/hr)	105·2
Solvent flow rate	(ml/hr)	145·6
Injection rate: benzene	(g/hr)	13·15
*cyclo*hexane	(g/hr)	11·57
Gas phase concentrations: benzene at feed point	(g/cm³)	$5{\cdot}6 \times 10^{-5}$
*cyclo*hexane at feed point	(g/cm³)	$7{\cdot}8 \times 10^{-5}$
benzene in top product	(g/cm³)	1×10^{-7}
*cyclo*hexane in top product	(g/cm³)	$1{\cdot}1 \times 10^{-4}$

Because of the high solvent concentrations and isothermal conditions existing above the feed point it was reasonable to assume that the equilibrium relationship was linear. Also the operating line for the benzene is linear when concentration are expressed in the units shown.

The value of N_G between the top of the column and the feed point by equation (3) was found to be 29·9 for the conditions given in Table 4, which corresponds to an H_G value of 2·2 cm. This method was not applied to the section of the column below the feed point because of the unknown temperature gradients there.

Acknowledgements—The authors wish to thank Professor S. R. M. Ellis for his continued interest and advice throughout this work. D. Critcher wishes to thank the Department of Scientific and Industrial Research for the provision of a research scholarship.

Nomenclature

A_L = cross-sectional area occupied by the mobile phase cm²
A_S = cross-sectional area occupied by the stationary phase (cm²)
R = retention time to centre of zone (min)
z = length of column (cm)
V_R = retention volume to centre of zone (ml)
p_i = pressure at column inlet (mm Hg)
p_0 = pressure at column outlet (mm Hg)
k = partition coefficient
L = solvent flow (l/hr)
G = air flow (l/hr)
H_G = height of a gas film transfer unit (cm)
H_{OG} = height of an over-all gas phase transfer unit (cm)
N_G = number of gas film transfer units
N_{OG} = number of over-all gas phase transfer units
y = concentration of component in gas phase (g/m³)

Subscripts

A = component A
B = component B
1 = concentrated end of countercurrent system
2 = dilute end of countercurrent system
e = equilibrium value
L.M. = logarithmic mean

Superscripts

R = rectification section
S = stripping section
F = feed point

References

[1] Ambrose D. and Collerson R. R. *Nature, Lond.* 1956 **177** 84.

[2] Atkinson E. P. and Tuey G. A. P. *Gas Chromatography* (Edited by Desty D. H.) p. 270. Butterworths, London 1958.

[3] Evans D. E. M. and Tatlow J. C. *Vapour Phase Chromatography* (Edited by Desty D. H.) p. 256. Butterworths, London 1957.

[4] Kirkland J. J. *Gas Chromatography* (Edited by Coates V. J.) p. 203. Academic Press, New York 1958.

[5] Podbielniak, Inc., Chicago, Illinois.

[6] Klinkenberg A. *Vapour Phase Chromatography* (Edited by Desty D. H.) p. 375. Butterworths, London 1957.

[7] Scott R. P. W. *Gas Chromatography* (Edited by Desty D. H.) p. 287. Butterworths, London 1958.

[8] Berg C. *Chem. Engng. Progr.* 1951 **47** 585.

[9] Freund M., Benedek P. and Szepesy L. *Vapour Phase Chromatography* (Edited by Desty D. H.) p. 359. Butterworths, London 1957

[10] Jamus A. T. and Martin A. J. P. *Analyst* 1952 **77** 915.

Chemical Engineering Science, 1960, Vol. 13, pp. 90 to 92. Pergamon Press Ltd., London. Printed in Great Britain

Letters to the Editors

Effects of sonic vibrations on the rate of absorption of gases from bubble beds

It is well known that bubbles produced at jets and in boiling liquids emit characteristic sounds. Minnaert [1] first analysed the sounds of bubbles produced at jets under various liquids and concluded that most of the sound was produced by radial pulsation of the bubble. Shortly afterwards Smith [2] considered the reverse effect – the vibration of bubbles produced by sound generated in the liquid – and concluded that the bubbles should show a high degree of resonance since the damping coefficient was small. He also suggested that the intense local strains in the vicinity of a pulsating bubble might account for the destructive effects of sound on vegetation and other living matter. In this connexion Ackerman [3] has shown that acoustic vibrations in the frequency range 0·4–500 kc/s can destroy Paramecia and Mammalian erythrocytes. The cavitation which destroyed the cells was ascribed to the presence of extremely small bubbles. Cavitation induced by sonics and ultrasonics in liquids has also been discussed by Rust [4], Kapustin [5] and Meyer [6]. In view of the above work it seemed likely that bubble vibration phenomena could be used to improve mass and heat transfer in operations such as gas absorption and boiling. As part of an initial study in this field we have studied the effect of sonic vibrations on the absorption of carbon dioxide from bubbles in water.

The apparatus is a modification of that described by Houghton *et al.* [7] and is shown in Fig. 1. The gas and liquid phases continuously enter and leave the top of a 2 ft length of 3 in. diameter glass pipe. The bottom of the column contains a closely fitting polystyrene piston sealed by a rubber diaphragm. The piston was vibrated by an electrodynamically driven vibrator at frequencies in the range 20–2000 c/s. The amplitude of the vibrations could be measured at each frequency by means of a microscope. A plot of amplitude against frequency is shown in Fig. 2. In order to avoid the effects of inert gases on the rate of absorption pure carbon dioxide was used. The gas was distributed in the liquid by a sintered glass candle of medium porosity. The rate of absorption was calculated in terms of $K_L a$ by measuring the inlet and outlet gas and liquid rates and also by analysing the liquid phase for dissolved carbon dioxide.

Fig. 2 shows the effects of frequency and amplitude on the rate of absorption of carbon dioxide in water as measured by the $K_L a$. The measurements were made at constant temperature, pressure, bed height, gas flow rate and liquid flow rate. It is evident from the data that the rate of absorption can be increased by as much as 50 per cent when certain vibration frequencies are used to excite the bubble bed. The greatest effect is at about 75 c/s.

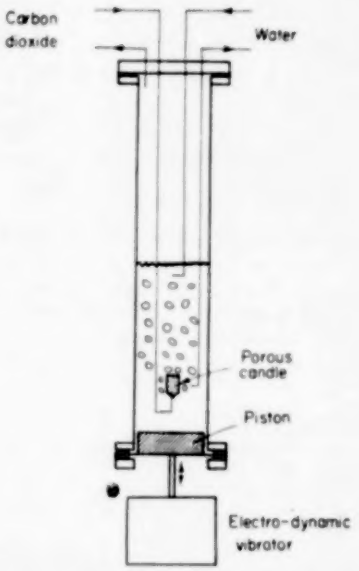

Fig. 1. Equipment.

The fact that the absorption rate shows peaks at certain frequencies together with the relatively small amounts of power introduced into the liquid (less than 4 W at all frequencies) indicates that the phenomena are due to resonance effects. The plot of amplitude vs. frequency for the case where no bubbles are present shows that peaks in amplitude cannot be the cause of the peaks in absorption rate. In most cases the peaks in absorption rate occur when the power input to the liquid is decreasing or relatively constant. Resonance effects are also indicated by the fact that the amplitude of the forcing vibration is somewhat dependent upon whether bubbles are present in liquid or not, as shown in Fig. 2. This effect is also quite audibly noticeable. When bubbles are introduced while the column of liquid is being vibrated, the presence of bubbles seems to strikingly increase or diminish (depending on the frequency) the volume of sound heard. Whether the effect as measured by $K_L a$ is due to a change in film coefficient for the individual bubbles or due to a change in area for absorption is not clear at the moment. However, visual observations on the effects of sound on single bubbles show that the sound can greatly affect their appearance. For instance, at low frequencies (20–60 c/s) the effect of sound appears to elongate the

VOL. 13 1961

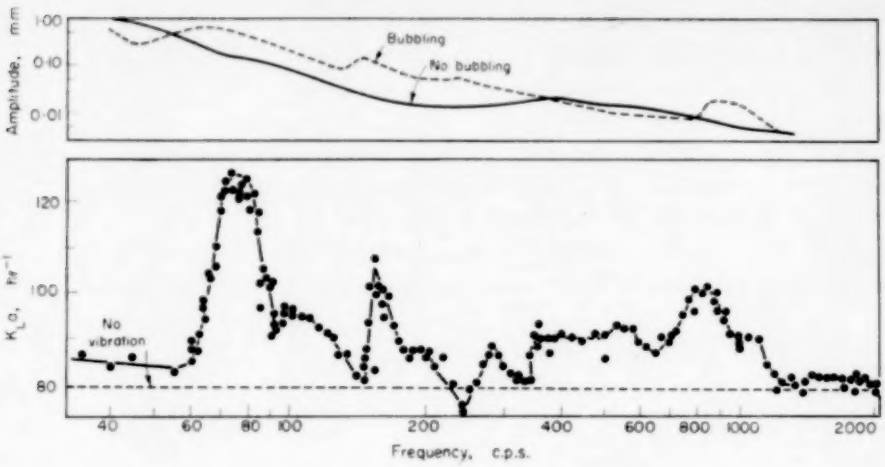

FIG. 2. Effect of frequency and amplitude on $K_L a$ for CO_2 in water. Pressure = 730 mm Hg. Temperature = 15°C. Inlet superficial gas velocity = 0·050 ft/sec. Water velocity = 0·040 ft/sec. Bed height = 1·0 ft.

bubbles in the direction of vibration while at higher frequencies (800–1200 c/s) the effect of the sound is to considerably disturb the bubble boundary to such an extent that the bubble takes on a frothy appearance. Intermediate frequencies (40–800 c/s) seem to have little effect on the appearance of single bubbles but greatly affect the appearance of the bubble bed, especially at the intermediate peaks shown in Fig. 2. For instance, at the peak of 75 c/s the visual effect of the sound is to produce turbulence and coalescence in the bubble bed. At the surface of the liquid the bubbles burst with some violence. Possibly these effects are caused by the presence of pressure nodes and antinodes as discussed by GOLDMAN and RINGO [8] and also BLAKE [9]. It is believed that the peak at about 840 c/s shown in Fig. 2 might correspond to the pulsation frequency of MINNAERT [1]. Since the pulsation frequency depends upon the diameter of the bubbles the average diameter of the bubbles in the bed can be calculated from MINNAERT's formula below:

$$f = \frac{656}{D}$$

where f is the frequency in c/s and D is the bubble-diameter in cm. The diameter corresponding to 840 c/s would be 7·8 mm. This is a much larger diameter than that usually found under similar conditions without the presence of sound [7] thus indicating that the sound may have produced coalescence of bubbles in the bed, thereby reducing the area for mass transfer. If this is the case the film coefficient must have increased considerably in order to produce an over-all increase in $K_L a$. The effect of sound on the coalescence of bubbles is discussed by BLAKE [9], who points out that two bubbles would be attracted to each other if their oscillations were in phase and repulsed if their oscillations were out of phase. It is possible that excessive coalescence might have caused $K_L a$ to decrease below the $K_L a$ for no vibration shown at 240 c/s in Fig. 2. The presence of peaks at low frequencies indicates that bubbles can vibrate in modes other than pulsation. However, the peaks at 145 and 280 c/s may be overtones of the peak at 75 c/s since they are of smaller intensity. Recent work by KOSTELLA [10] and SKLENCAR [11] using a wave-analyser has confirmed the existence of the pulsation frequency of MINNAERT, but has shown that frequencies other than the pulsation frequency can be emitted from single bubbles formed at a jet. Although these workers did not make measurements below 200 c/s they found other frequencies that could not be attributed to pulsation, particularly in the range 400–600 c/s. Although no attempt was made to attribute these frequencies to definite modes of vibration, they may account for the generally high level for the absorption rate in the 400–600 c/s region shown in Fig. 2.

Chemical Engineering Department K. L. HARBAUM
Division of Engineering Research G. HOUGHTON
University of Pittsburgh

REFERENCES

[1] MINNAERT M. *Phil. Mag.* 1933 **16** 235.
[2] SMITH F. D. *Phil. Mag.* 1935 **19** 1147.

[3] Ackerman E. *J. Appl. Phys.* 1953 **24** 1371.

[4] Rust H. H. *Angew. Chem.* 1953 **65** 249.

[5] Kapustin A. P. *Zh. Tekh. Fiz.* 1954 **24** 1008.

[6] Meyer E. *J. Acoust. Soc. Amer.* 1957 **29** 4.

[7] Houghton G., McLean A. M. and Ritchie P. D. *Chem. Engng. Sci.* 1957 **7** 26, 40.

[8] Goldman D. E. and Ringo G.R. *J. Acoust. Soc. Amer.* 1949 **21** 270.

[9] Blake F. G. *J. Acoust. Soc. Amer.* 1949 **21** 551.

[10] Kostella R.M. *The Acoustics of Bubbles*, M.S. Thesis, University of Pittsburgh 1958.

[11] Sklencar A. M. *Effect of Physical Properties on the Acoustics of Bubbles*, M.S. Thesis, University of Pittsburgh 1959.

VOL.
13
1961

Chemical Engineering Science, 1960, Vol. 13, p. 93. Pergamon Press Ltd., London. Printed in Great Britain

Book Reviews

F. C. VILBRANDT and C. E. DRYDEN: **Chemical Engineering Plant Design.** (Fourth Edition – revised). McGraw-Hill, New York 1959. 534 pp. 80s., $12.00.

SINCE the inital publication of *Chemical Engineering Plant Design* by F. C. VILBRANDT in 1934, this book has been widely used through three editions as both a text and a reference work for plant design in the process industries.

The fourth edition, under the co-authorship of F. C. VILBRANDT and C. E. DRYDEN, presents a considerable departure, both in content and arrangement, from the previous editions. Information is presented in approximately the same chronological order as it is required for the actual design of a chemical plant, beginning with a consideration of development of the project, and proceeding through process design, equipment and materials selection, plant layout, economic evaluation, plant location, and site preparation and structures. The volume is arranged so the more detailed material, such as plant layout and location, may be omitted without hindering the presentation of other subject matter.

All cost data have been brought up-to-date, and quite a few references dealing with recent developments in cost estimation techniques and equipment selectiun have been added since the last edition. All references for collateral reading have been placed together at the end of the text material, rather than at the end of each chapter.

The rearrangement of the order of presentation of material undoubtedly has proxided a substantial improvement in the book; however, there are a few specific criticisms. Of the topics presented, the section on economic evaluation is least satisfying, since the general subject is dealt with at considerable length but only the most simple concepts are presented quantitatively. A description of the economics of selecting alternates would be of particular value, as would be a more detailed consideration of the time value of money in economic calculations. The one entirely new section included in the fourth edition deals with nuclear chemical plant design, covering primarily shielding and criticality calculations. Both subjects are treated more quantitatively and with more detail elsewhere.

The reviewer feels that the present edition is much clearer in presentation of material than previous editions. the thoroughness in coverage of cost estimation methods and data, together with the logical and clear presentation of the general problem of chemical plant design, make the book one to be recommended. J. B. BUTT

SELECTION OF CURRENT PAPERS OF INTEREST TO CHEMICAL ENGINEERS

OLE LAMM: Diffusion coefficient and friction in a general two-component fluid. *Trans. Farad. Soc.* 1960 **56** 767–769.

P. H. THOMAS: Some approximations in the theory of self-heating and thermal explosion (Solutions of conduction equations with terms owing to chemical reaction). *Trans. Farad. Soc.* 1960 **56** 833–839.

R. M. BARRER and T. GABOR: Sorption and diffusion of simple paraffins in silica-alumina cracking catalyst. *Proc. Roy. Soc.* 1960 **A256** 267–290.

M. L. LIGHTHILL: Dynamics of a dissociating gas. Part 2. Quasi-equilibrium transfer theory (see also: *J. Fluid Mech.* 1957 **2** 1). *J. Fluid Mech.* 1960 **8** 161–182.

B. R. MORTON: Laminar convection in uniformly heated vertical pipes. *J. Fluid Mech.* 1960 **8** 227–240.

C. HUNTER: On the collapse of an empty cavity in water. *J. Fluid Mech.* 1960 **8** 241–263.

P. G. SAFFMAN: On the effect of molecular diffusivity in turbulent diffusion. *J. Fluid Mech.* 1960 **8** 273–283.

L. M. MACK: The compressible viscous heat-conducting vortex. *J. Fluid Mech.* 1960 **8** 284–292.

K. V. KRISHNA RAO: Simple method of determining the thickness or the refractive index of thin films. *Amer. J. Phys.* 1960 **28** 447–449.

T. H. RICHARDS: Analogy between the slow motion of a viscous fluid and the extension and flexure of plates: a geometric demonstration by means of moiré fringes. *Brit. J. Appl. Phys.* 1960 **11** 244–254.

G. NYUL and E. VAMOS: Refining of lubricating oils by chromatography. *J. Inst. Petrol.* 1960 **46** 101–108.

R. F. CROUCH and A. CAMERON: Graphical integration of the Maxwell fluid (viscosity depends on pressure) equation and its application. *J. Inst. Petrol.* 1960 **46** 119–125.

G. A. GILBERT: Concentration-dependent sedimentation of aggregate proteins in the ultracentrifuge. *Nature Lond.*, 1960 **186** 882–883.

VOL 13 1961

SELECTION OF CURRENT SOVIET PAPERS OF INTEREST TO CHEMICAL ENGINEERS*

YA. G. GOROSHCHENKO, V. I. BELOKOSKOV and A. G. BABKIN: Distribution of rare earth elements between solid and liquid phases in crystallization of double sulphates. *Zh. prikl. Khim.* 1960 **33** 803–808.

I. N. KUZMINIKH and A. G. KUZNETSOVA: Equilibrium between pyridine vapour and acidic solutions of pyridine sulphate. *Zh. prikl. Khim.* 1960 **33** 865–870.

V. P. SUMAROKOV and Z. M. BOLUDUTSKAYA: Distribution of furfural between water and some organic solvents. *Zh. prikl. Khim.* 1960 **33** 910–914.

A. M. GINSTLING and A. A. BARAM: Application of ultrasound in processes of chemical technology. *Khim. Prom.* 1960 (1) 9–19.

M. G. SLINKO: On the role of mass transfer in catalytic oxidation of naphthalene to phthalic anhydride *Khim Prom.* 1960 (1) 24–25.

F. YA. REVZIN: On the problem of purification of technical gases from hydrogen sulphide and carbon dioxide. *Khim. Prom.* 1960 (1) 48–51.

YA. I. TURYAN and N. S. ANIKINA: Method of automatic control of alkaline absorption of nitrogen oxides in the manufacture of weak nitric acid. *Khim. Prom.* 1960 (1) 59–61.

M. A. AEROV, T. A. BYSTROVA, E. P. DAROVSKIKH and L. E. SUM-SHIK: Tubular grid-type plates. Hydraulic resistance, effectiveness and heat transfer. *Khim. Prom.* 1960 (1) 62–66. The plate consists of a tube coiled into a spiral.

A. G. KASATKIN and YU. I. DITNERSKI: On selection of flow rates in plate columns. *Khim. Prom.* 1960 (1) 66–69.

YU. K. MOLOKANOV: On the size of slot opening in a bubble-cap. *Khim. Prom.* 1960 (1) 69–73.

D. S. TSIKLIS, L. I. SHENDEREI and A. N. KOFMAN: Solubility of acetaldehyde in compressed gases. *Zh. fiz. Khim.* 1960 **34** 768–772.

N. U. KOIDA: Application of the similarity principle to the filtration of liquids. *Zh. fiz. Khim.* 1960 **34** 789–794.

A. G. USMANOV and A. N. BEREZHNOI: Application of the theory of similarity to studies of mass transfer. *Zh. fiz. Khim.* 1960 **34** 907–920.

V. I. KUTUKOVA, E. V. VOZNENSKAYA and R. K. STOYANOVICH: Rotary disc contactor for purification of lubricating oil fractions by furfural. *Khim. Tekh. Topl. Masel* 1960 **5** (5) 16–21.

N. I. GAMAYUNOV: Investigation of the transfer of heat and mass in a finite rod. *Inzh.–Fiz. Zh.* 1960 **3** (4) 11–17.

N. G. ZALOGIN, F. E. KENEMAN and V. N. VOROBYEV: The mechanism of free efflux of granular materials—II. *Inzh.–Fiz. Zh.* 1960 **3** (4) 18–22.

I. L. KAROL: A semi-empirical theory of vertical eddy diffusion in the boundary layer of the atmosphere. *Inzh.–Fiz. Zh.* 1960 **3** (4) 54–64.

R. A. VOLKOV: Application of Laplace transforms to certain hydrodynamic problems. *Inzh.–Fiz. Zh.* 1960 **3** (4) 65–72. Solution of Stokes–Navier equation in the Oseen approximation for flow from a round opening at the bottom of a tank and for flow from a round pipe.

G. D. RABINOVICH: Certain problems of non-steady heat transfer in a bed of granular material. *Inzh.–Fiz. Zh.* 1960 **3** (4) 73–80.

V. Y. FRENKEL: Heat exchange by radiation between two parallel infinite cylinders. *Inzh.–Fiz. Zh.* 1960 **3** (4) 85–89.

*To assist readers, translations of any article appearing in the above list can be obtained at a reasonable charge. All orders should be addressed to the Administrative Secretary of the Pergamon Institute at either Headington Hill Hall, Oxford or 122 East 55th Street, New York 22, whichever is more convenient.

V. S. Ermakov: Non-steady temperature field in heating elements of a reactor. *Inzh.-Fiz. Zh.* 1960 **3** (4) 127–131.

I. V. Petukhov: Numerical integration of equations for a laminar boundary layer. *Dokl. Akad. Nauk SSSR* 1960 **132** 307–310.

D. A. Efros: Permeability of porous media to gasified fluid. *Dokl. Akad. Nauk SSSR* 1960 **132** 311–314.

E. F. Kurgaev: On the viscosity of suspensions. *Dokl. Akad. Nauk SSSR* 1960 **132** 392–394.

D. A. Efros and I. F. Kuranov: Calculation of flow of gasified liquids with a two-parameter characteristics of permeability. *Dokl. Akad. Nauk SSSR* 1960 **132** 553–556.

G. A. Tirski: Surface melting of a semi-infinite body in either a plane or axially symmetrical incompressible gas flow. *Dokl. Akad. Nauk SSSR* 1960 **132** 785–788.

B. S. Petukhov and V. V. Kirillov: Heat transfer in turbulent flow of compressed gas in pipes at compressibilities from 0·5 to 4. *Teploenergetika* 1960 **7** (5) 64–72.

B. I. Levin: Heat transfer in condensation of saturated steam on the surface of a vertical bundle of tubes. *Teploenergetika* 1960 **7** (5) 73–75.

D. A. Labuntsov: Generalized correlation for heat transfer in nucleate boiling of liquids. *Teploenergetika* 1960 **7** (5) 76–81.

VOL. 13 1961